NATIONAL ADVISORY COMMITTEE FOR AERONAUTICS

TECHNICAL NOTE

No. 1491

THEORETICAL ADDITIONAL SPAN LOADING CHARACTERISTICS OF WINGS WITH ARBITRARY SWEEP, ASPECT RATIO, AND TAPER RATIO

By John DeYoung

Ames Aeronautical Laboratory
Moffett Field, Calif.

Washington
December 1947

NATIONAL ADVISORY COMMITTEE FOR AERONAUTICS

TECHNICAL NOTE NO. 1491

THEORETICAL ADDITIONAL SPAN LOADING CHARACTERISTICS OF WINGS WITH ARBITRARY SWEEP, ASPECT RATIO, AND TAPER RATIO

By John DeYoung

SUMMARY

The Weissinger method for determining additional span loading has been used to find the lift-curve slope, spanwise center of pressure, aerodynamic center location, and span loading coefficients of untwisted and uncambered wings having a wide range of plan forms characterized by various combinations of sweep, aspect ratio, and taper ratio. The results are presented as variations of the aerodynamic characteristics with sweep angle for various values of aspect ratio and taper ratio. Methods are also included for determining induced drag and the approximate effects of compressibility.

Despite the limitations of a lifting line method such as Weissinger's, the good agreement found between experimentally and theoretically determined characteristics warrants confidence in the method. In particular, it is believed that trends observed in results of the Weissinger method should be reliable. One of the most significant results showed that for each angle of sweep there is a taper ratio for which aspect ratio has little effect on the span loading and for which the loading is practically elliptical. This elliptic loading is approached at a taper ratio of 1.39 for 30° of sweepforward, 0.45 for 0° of sweep, and 0.14 for 30° of sweepback.

INTRODUCTION

In an effort to overcome the many problems posed by transonic and supersonic flight speeds, a number of unconventional wing plan forms have been considered for use. The characteristics of most of these unconventional wings are as yet largely undetermined. The multiplicity of possible plan forms has made it difficult to conduct a comprehensive experimental study and until fairly recently no adequate theoretical approach was possible. Several newly developed methods for computing the low-speed characteristics of wings having other than conventional plan forms were compared and their accuracy

evaluated in reference 1. It was concluded from this study that the theoretical method developed by Weissinger for computing the span load (and associated characteristics) of wings was well suited for an over-all study of the effects of wing plan form.

This report has therefore been prepared in which for additional loading the Weissinger method has been used to compute the lift-curve slope, spanwise center of pressure location, aerodynamic center location (based on spanwise center of pressure change due to sweep), and span-loading variation for a series of wings encompassing the probable ranges of sweep angle, taper ratio, and aspect ratio. The range of plan forms considered is shown on figure 1. This figure does not show all of the plan forms for which computations were made but does serve to give approximately the limits considered. In the limited number of cases possible, experimental data, other than that reported in reference 1, have been used to verify the correctness of the computations.

SYMBOLS

Aerodynamic Parameters

$\frac{c_l c}{C_L c_{av}}$	spanwise loading coefficient
$\frac{c_l}{C_L}$	ratio of local lift coefficient to wing lift coefficient
$\frac{dC_L}{d\alpha}$	lift-curve slope at zero lift
$\frac{C_{D_i}}{C_L^2}$	rate of change of induced drag with squared lift coefficient
η_{cp}	spanwise center of pressure location on one wing panel, fraction of semispan $[y_{cp}/(b/2)]$
a.c.	aerodynamic center location measured in percent of the centroid-of-area chord from leading edge of the centroid-of-area chord
c_l	local lift coefficient $\left(\frac{\text{local lift}}{qS}\right)$

C_L	wing lift coefficient $\left(\frac{\text{total lift}}{qS}\right)$
α	angle of attack, degrees
Γ	circulation, feet squared per second
q	free-stream dynamic pressure, pounds per square foot
M	Mach number

Geometric Parameters

$\Lambda_{c/4}$	sweep angle of the quarter-chord line, positive for sweepback, degrees
A	aspect ratio $\left(\frac{b^2}{S}\right)$
λ	taper ratio $\left(\frac{\text{tip chord}}{\text{root chord}}\right)$
S	wing area, square **feet**
c	wing chord parallel to plane of symmetry, feet
c_{av}	mean wing chord $\left(\frac{S}{b}\right)$ feet
c_r	root chord, feet
C.A.C.	centroid-of-area chord $\left(\frac{\int_{-1}^{+1} c^2 \, d\eta}{S}\right)$
t	fraction of chord measured from leading edge of the wing chord
x	longitudinal coordinate measured from leading edge of root chord and parallel to the plane of symmetry, **positive** to the rear, feet
b	wing span perpendicular to the plane of symmetry, feet
y	lateral coordinate measured from wing root perpendicular to the plane of symmetry, positive to the right, feet
η	dimensionless lateral coordinate $\left(\frac{y}{b/2}\right)$

φ trigometric spanwise coordinate having a value varying from 0 at b/2 to π at -b/2, $(\cos^{-1} \eta)$, degrees

η_n, η_k dimensionless lateral coordinates at specific span stations designated by the integers n and k in the relationships $\eta_n = \cos \frac{n\pi}{8}$ and $n_k = \cos \frac{k\pi}{16}$, respectively

μ_1 series integers

a_{nk} interpolation factors for additional span loading coefficients

Subscripts

n, k integers defining specific span locations

e equivalent

L.E. leading edge

T.E. trailing edge

t fraction of local chord

PROCEDURE

The Weissinger method replaces the spanwise load by a line vortex located at the swept quarter-chord position. The spanwise strength variation of the line vortex is determined by the boundary conditions that there can be no flow through the mean camber line at the three-quarter chord point, or in effect, that the ratio of vertical induced velocity (due to bound vortex and trailing vortex sheet) to free-stream velocity be equal to the slope of the mean camber line at the three-quarter-chord point. The theory thus is applicable for various plan forms that can have camber and twist. Generally, however, it is considered most expedient to determine the loading of a wing by finding the basic loading due to camber and twist and adding to this the additional loading due to angle of attack to obtain the total loading. This report confines itself to a treatment of the additional load. In reference (1) sufficient information is given to obtain by the Weissinger method the basic loading of a wing having camber and twist.

Procedure for the Characteristics Presented

Lift-curve slope, spanwise center of pressure, and span loading coefficients.- The Weissinger method and a shortened computing form, amply presented in appendix C of reference (1), is the procedure followed for calculating lift-curve slope $dC_L/d\alpha$, spanwise center of pressure η_{cp}, and the span loading coefficients $c_l c/C_{L c_{av}}$ presented herein.

Aerodynamic center.- The Weissinger method may be extended to give a good approximation of the position of the aerodynamic center (a.c.) with respect to a reference chord for wings having moderate to great angles of sweep. The approximation arises from the fact Weissinger considers the loading concentrated along the quarter-chord line which is, of course, not strictly correct. However, it is apparent that as the wing is increasingly swept, the longitudinal location of the aerodynamic center with regard to a reference chord becomes increasingly a function of the spanwise location of center of pressure and hence relatively less a function of the chordwise loading. Because the Weissinger method gives an accurate prediction of the spanwise center of load, it follows that it should give a good prediction of the longitudinal position of the aerodynamic center of wings having appreciable sweep.

For wings the plan form of which can be precisely defined by taper ratio, aspect ratio, and sweep, the following expression can be derived which locates the fore and aft position of the aerodynamic center on the centroid-of-area chord[1] and involves a knowledge

---

[1]Centroid-of-area chord as used herein is defined as the ratio of the mean square chord to the mean chord or,

$$C.A.C. = \frac{\int_{-1}^{1} c^2 \, d\eta}{\int_{-1}^{1} c \, d\eta} = \frac{\int_{-1}^{1} c^2 \, d\eta}{S}$$

This chord which passes through the centroid-of-area of the wing plan form is the true mean aerodynamic chord for uniform spanwise section lift coefficient c_l distribution. For unswept and moderately swept wings of conventional plan forms the centroid-of-area chord is so nearly coincident with the true M.A.C. that the substitution is acceptable. The substitution becomes increasingly in error as the spanwise section lift-coefficient distribution departs from a uniform distribution as in the case of highly swept wings. It is for this reason that throughout this report the reference chord used has been called the centroid-of-area chord (C.A.C.)

---

only of the aforementioned wing geometry parameters and the predicted spanwise center of load.

$$a.c. = \frac{1}{4} + \frac{3(1+\lambda)^2}{8(1+\lambda+\lambda^2)} \left[\eta_{cp} - \frac{1+2\lambda}{3(1+\lambda)} \right] A \tan \Lambda_{c/4} \qquad (1)$$

Procedures for Additional Characteristics

Included in this section are procedures for determining additional wing characteristics using the data presented in this report. It was believed that these characteristics did not warrant detailed presentation but that inclusion of simple procedures for their determination would increase the usefulness of the data presented.

Local lift coefficient and induced drag.- With the loading coefficient known the local lift coefficient may be obtained by

$$\frac{c_l}{C_L} = \left(\frac{c_l c}{C_L c_{av}} \right) \left(\frac{c_{av}}{c} \right)$$

$$= \left(\frac{c_l c}{C_L c_{av}} \right) \left\{ \frac{1+\lambda}{2[1-\eta(1-\lambda)]} \right\} \qquad (2)$$

The induced drag coefficient can also be obtained when the span-loading coefficients are known (reference 2).

Let $K_n = \left(\frac{c_l c}{C_L c_{av}} \right)_n$

where the n's are integers giving the spanwise stations through the relationship $\eta = \cos n\pi/8$. (That is, when $n = 1, 2, 3, 4$, $\eta = 0.9239$, 0.7071, 0.3827, 0, respectively.) Then the induced drag is given by

$$\frac{C_{D_i}}{C_L^2} = \frac{\pi}{8A} \left[K_1^2 + K_2^2 + K_3^2 + \frac{K_4^2}{2} \right.$$

$$- K_4 (0.0561 K_1 + 0.7887 K_3)$$

$$\left. - K_2 (0.7352 K_1 + 0.8445 K_3) \right] \qquad (3)$$

Effects of compressibility.- Recent British work by Dickson in an application of the Prandtl-Glauert rule has resulted in a method for predicting the effects of compressibility below critical speed on the span loading of swept wings. Experimentally determined compressibility effects on loading have not been compared as yet with results given by this method; therefore the method should be used with caution until such comparisons are made, especially where viscous effects might be important.

The method may be summarized as follows:

The lift distribution of an airfoil at a given Mach number is obtained by calculating the lift distribution in incompressible flow of an equivalent airfoil the lateral dimensions of which have been reduced in the ratio $\sqrt{1-M^2} : 1$. The aspect ratio is thus reduced in this ratio and the tangent of sweep angle is increased by $\frac{1}{\sqrt{1-M^2}}$. The dimensions of the equivalent wing become

$$\lambda_e = \lambda$$

$$A_e = \sqrt{1-M^2}\, A \tag{4}$$

$$\left(\tan \Lambda_{c/4}\right)_e = \frac{\tan \Lambda_{c/4}}{\sqrt{1-M^2}}$$

Using the equivalent parameters, values of the aerodynamic characteristics are obtained from the charts and are then multiplied by the factors in the following table:

Aerodynamic characteristics	Factor
$dC_L/d\alpha$	$\frac{1}{\sqrt{1-M^2}}$
$C_{D_i}/C_L{}^2$	$\sqrt{1-M^2}$
Center of spanwise pressure	1
c_l/C_L	1
Center of chordwise pressure	1

Sweep-Angle Conversion Formulas

Unless specifically stated otherwise, the sweep angle used throughout the present report is the angle of sweep of the quarter-chord line. The following equation, easily derived from wing geometry, gives the sweep of any chord line in terms of the sweep of the quarter-chord line, the taper ratio, and aspect ratio:

$$\tan \Lambda_t = \tan \Lambda_{c/4} - \frac{4(t-0.25)}{A}\left(\frac{1-\lambda}{1+\lambda}\right) \tag{5}$$

When $t = 0$, Λ_0 = the sweep at the leading edge $\Lambda_{L.E.}$

$$\text{or} \quad \tan \Lambda_{L.E.} = \tan \Lambda_{c/4} + \frac{1}{A}\left(\frac{1-\lambda}{1+\lambda}\right) \tag{6}$$

When $t = 1$, Λ_1 = the sweep at the trailing edge, $\Lambda_{T.E.}$

$$\text{or} \quad \tan \Lambda_{T.E.} = \tan \Lambda_{c/4} - \frac{3}{A}\left(\frac{1-\lambda}{1+\lambda}\right) \tag{7}$$

The relationship between the wing parameters for the straight trailing-edge wings is given by equation (7) for $\Lambda_{T.E.} = 0$

$$\text{or} \quad \tan \Lambda_{c/4} = \frac{3}{A}\left(\frac{1-\lambda}{1+\lambda}\right) \tag{8}$$

Further, when $\lambda = 0$ in equation (8), the relationship between $\Lambda_{c/4}$ and A for the triangular wing is obtained, that is,

$$\tan \Lambda_{c/4} = \frac{3}{A} \tag{9}$$

RESULTS AND DISCUSSION

Aerodynamic Characteristics

The results of applying the Weissinger method to determine the additional loading characteristics of the wide range of plan forms shown in figure 1 are presented in figures 2,3, 4, and 5.

In figure 2 the variation of lift-curve slope $dC_L/d\alpha$ with sweep of the quarter-chord line is shown for a family of aspect

ratios and given values of taper ratio. For two-dimensional wings ($A = \infty$) the variation of lift-curve slope with sweep angle is given by $\frac{dC_L}{d\alpha} = \frac{2\pi}{57.3} \cos \Lambda_{c/4}$. This curve is included in figure 2 as a limiting aspect ratio. Also shown in figure 2 are lines indicating plan forms with $\Lambda_{L.E.} = 0$ and $\Lambda_{T.E.} = 0$ (from equations (6) and (7)) to segregate the ranges of plan forms.

The variations of spanwise center of pressure η_{cp} and aerodynamic center a.c. (from equation (1)) with $\Lambda_{c/4}$ are shown in figures 3 and 4 for families of aspect ratios and given taper ratios.

Similarly the loading coefficients $\frac{c_l c}{C_L c_{av}}$ are presented in figure 5 for spanwise stations $\eta = 0$, 0.3827, 0.7071, and 0.9239. The loading coefficients are obtained as four values for the corresponding four spanwise stations. If more than four values of loading are required to fair the loading curve, additional points may be obtained through the use of a simple loading series. (See Appendix.)

Comparison of Theoretical and Experimental Results

In reference 1 the Weissinger method was applied to five swept wings for which experimental data were available. A comparison of the predicted and measured results showed reasonably good agreement. However, since the plan forms included in the present investigation varied considerably from those reported in reference 1, additional checks were desired to evaluate the Weissinger method. A number of comparisons with respect to lift-curve slope, spanwise loading and aerodynamic center location are presented in figures 6, 7, and 8.

Figure 6(a) compares the variation with aspect ratio of the lift-curve slope for elliptic wings as given by references 3 and 4 with the lift-curve slope of wings having a 0.4 taper ratio as predicted by the Weissinger method. It is generally conceded that the values given by references 3 and 4 are quite accurate. The 0.4 taper ratio wing was chosen for comparison since it shows nearly elliptic loading. It can be seen that the Weissinger method predicts the effects of aspect ratio as accurately as the best methods otherwise available. It is of interest to note that the three methods predict the same variation of lift-curve slope at very low aspect ratios as does reference 5.

Experimental data exist on two series of wings having a constant plan form but varying aspect ratio. Reference 6 shows the effect of aspect ratio on the lift-curve slope of rectangular wings, and

reference 7 shows the effect of aspect ratio on the lift-curve slope of triangular wings. Figure 6(b) has been prepared to show how well the Weissinger method predicts the experimental variation. The agreement shown is considered good.

To show the ability of the method to predict the lift-curve slope of a wide variety of plan forms which did not vary consistently with any geometric parameter, figure 6(c) has been prepared. This compares predicted and measured lift-curve slopes for the wings reported in references 7 and 8. Here, too, the predictions appear good.

Experimental loading data were available for only one of the wings, the triangular wing of aspect ratio 2.0. In figure 7 the experimental and theoretical loading for this wing are compared and again excellent agreement is obtained.

To afford a comparison of experimentally and theoretically determined aerodynamic center locations, figure 8 has been prepared which correlates these locations for the wings considered in reference 8. Those models which had aspect ratios less than 1.5 or which included fuselages were excluded from the correlation, since they were beyond the range of this investigation. (Note that several models having stings were included.) Also excluded were the unswept wings because the Weissinger method inherently places the aerodynamic center at the quarter chord for these wings. With regard to the aerodynamic center location, experiment and theory do not show as good agreement as in the case of lift-curve slope and span loading. However, in considering the difficulty of precisely determining the aerodynamic center location from force tests, it is believed that the discrepancies in correlation shown in figure 8 are due in great part to experimental scatter and possibly viscous effects. The fact that there is no systematic variation in the correlation with variation in plan form serves to substantiate this belief. Therefore it is concluded that the method will give an acceptable value of aerodynamic center for wings having plan forms of the general type included in this correlation, that is, sweep greater than 15°, aspect ratio greater than 1.5.

Thus from the foregoing it can be stated that the Weissinger method will in general predict certain wing characteristics (C_{L_α}, η_{cp}, a.c., $c_l c/C_L \bar{c}$) with accuracy of the same order as that obtainable from experiment. In particular it is believed that the prediction of the incremental effects or trends in characteristics due to sweep, aspect ratio, or taper ratio are reliable.

Effect of Plan-Form Variation on Aerodynamic Characteristics

Examination of figure 2 reveals certain general trends with respect to the effect of wing plan form on wing lift-curve slope. For wings of high aspect ratio, the angle of sweep has a marked effect on lift-curve slope with the maximum effect occurring for wings of infinite aspect ratio when the lift-curve slope is directly a function of the angle of sweep. As the aspect ratio approaches very low values the lift-curve slope for the unswept wing is greatly reduced and the effects of sweep become small except for very large angles of sweep. Also it can be seen that at very large angles of sweep the effects of aspect-ratio variation on lift-curve slope become small.

To better illustrate the separate effects of aspect ratio and taper ratio, the data from figure 2 have been cross-plotted to show the variation with aspect ratio of the lift-curve slope for various values of taper ratio and sweep angle. These results are shown on figure 9(a). This shows clearly how increasing the angle of sweep decreases the variation of lift-curve slope with aspect ratio. It shows further that while taper ratio as compared to aspect ratio has only a small effect on the lift-curve slope of an unswept wing, taper ratio has a predominant effect on the lift-curve slopes of highly swept wings of moderate to high aspect ratios. For very small aspect ratios, however, the lift-curve slopes of all the wings converge and become almost a linear function of aspect ratio, being essentially independent of the effects of sweep and taper. This linear variation of lift-curve slope with aspect ratio was derived by R.T. Jones (reference 5) for the case of pointed wings but from these results it would appear to apply to low-aspect-ratio wings of any plan form. Figure 9(b) shows the effect of taper ratio on the variation of lift-curve slope with angle of sweep for a constant aspect ratio. The most significant fact shown by this figure is that as the taper ratio is increased from zero, the angle of sweep at which the maximum value of C_{L_α} occurs changes progressively from positive to negative angles of sweep.

In figure 4 variations of aerodynamic center location from 15 percent C.A.C. to 45 percent C.A.C. are indicated for the range of plan forms studied. It will be noted that for taper ratio $\lambda = 0$ the aerodynamic center moves aft for sweepback and forward for sweep-forward. At taper ratios of 1.0 and 1.5 the aerodynamic center moves forward for sweepback and aft for sweepforward. For $\lambda = 0$ the effects of aspect ratio are largely confined to the swept-back wings and as taper ratio is increased the effect of aspect ratio decreases on swept-back wings and increases for swept-forward wings. Where the effects of aspect ratio are significant, an increase in aspect ratio generally moves the aerodynamic center aft.

Figure 10 has been prepared from cross-plotting the data of figure 5 in order to show directly the effect of sweep and taper ratio on the span loading of a wing of constant aspect ratio of three. It shows that increasing the angle of sweepback or the taper ratio serves to move the loading (as defined by $c_l c/C_{L c_{av}}$) outboard. It is evident that the effects of taper are somewhat stronger for the more highly swept-back wing than for the highly swept-forward wing.

The spanwise center of pressure is independent of aspect ratio for certain combinations of taper ratio and sweep angle, as seen in figure 3. These values of taper ratio are plotted against sweep angle in figure 11. Further, for the wing geometry represented by the curve of figure 11 the loading is approximately independent of aspect ratio (fig. 5); and also is approximately elliptical. For elliptical loading, the loading coefficients at the four spanwise stations are 1.273, 1.176, 0.900, and 0.487. It can be seen that these values compare closely with values given in figure 5 for the plan forms specified in figure 11. The further the wing geometry departs from the configuration represented by the curve in figure 11, the greater the change of loading with aspect ratio and the rate of distortion from an elliptical load distribution. Also examination of figure 5 will show that elliptical loading cannot be obtained by altering aspect ratio alone; however, all wings approach an elliptical loading as aspect ratio approaches zero.

The wings of figure 11 have the property that their aerodynamic characteristics can be expressed in a simple manner similar to the case of unswept wings with elliptic plan forms. Namely, the induced drag is given approximately by $C_{D_i}/C_L^2 = 1/\pi A$, spanwise center of pressure by $\eta_{cp} = 4/3\pi$, and aerodynamic center location with respect to the centroid-of-area chord by $\text{a.c.} = \frac{1}{4} + \frac{0.342-0.567\lambda-0.908\lambda^2}{10(1+\lambda+\lambda^2)} A \tan \Lambda_{c/4}$.

From figure 2 it can be shown that the wings of figure 11 give the maximum lift-curve slope for a given aspect ratio and sweep angle.

In summary, the curve of figure 11 defines wings having the following approximate characteristics: span loading independent of aspect ratio, maximum lift-curve slope for a given sweep and aspect ratio, a constant spanwise center of pressure and an aerodynamic center location that is a simple function of wing geometry only.

Ames Aeronautical Laboratory,
National Advisory Committee for Aeronautics,
Moffett Field, Calif.

APPENDIX

MODIFICATION OF ANALYTICAL SERIES USED FOR SPAN LOADING BY THE WEISSINGER METHOD

The span loading series as originally presented by Weissinger is in a form which, due to the number of terms in the series, is too cumbersome for analytical application. Since in his method Weissinger avoided an analytical application of the series, and determined the circulation directly at four spanwise stations, he probably believed a short analytical expression was unnecessary. However, if only four values of loading are known, the fairing of these points becomes somewhat uncertain and a simple analytical expression is desirable. The results of simplifying the original loading series are presented in this appendix along with simple formulas and tables for interpolating additional span loading coefficients.

The circulation distributions from reference 9 (for m = 7) are given as

$$\Gamma(\varphi) = \frac{1}{4} \sum_{n=1}^{7} \Gamma_n \sum_{\mu_1=1}^{7} \sin \mu_1 \left(\frac{n\pi}{8}\right) \sin \mu_1 \varphi \qquad (A1)$$

In this equation $\Gamma(\varphi)$ is the value of the circulation at the variable span station φ, $(\varphi = \cos^{-1} \eta)$ and Γ_n is the circulation at the span station $\varphi_n (\varphi_n = \frac{n\pi}{8}$, where n is an integer).

Since $\Gamma \sim c_l c$, the series may be written in terms of a loading coefficient K defined by

$$K = \frac{c_l c}{C_L c_{av}}$$

Rewriting equation (A1) in terms of K gives

$$K(\varphi) = \frac{1}{4} \sum_{n=1}^{7} K_n \sum_{\mu_1=1}^{7} \sin \mu_1 \left(\frac{n\pi}{8}\right) \sin \mu_1 \varphi \qquad (A2)$$

This series may be simplified into any of the three following forms (for a symmetrical wing):

$$K(\varphi) = \sum_{n=0}^{3} a_{2n+1} \sin (2n+1)\varphi \qquad (A3)$$

where in terms of the coefficients [1] K_n

$$a_1 = \frac{1}{2}\left(\frac{K_4}{2} + K_3 \sin \frac{3\pi}{8} + K_2 \sin \frac{\pi}{4} + K_1 \sin \frac{\pi}{8}\right)$$

$$a_3 = \frac{1}{2}\left(-\frac{K_4}{2} - K_3 \sin \frac{\pi}{8} + K_2 \sin \frac{\pi}{4} + K_1 \sin \frac{3\pi}{8}\right)$$

$$a_5 = \frac{1}{2}\left(\frac{K_4}{2} - K_3 \sin \frac{\pi}{8} - K_2 \sin \frac{\pi}{4} + K_1 \sin \frac{3\pi}{8}\right)$$

$$a_7 = \frac{1}{2}\left(-\frac{K_4}{2} + K_3 \sin \frac{3\pi}{8} - K_2 \sin \frac{\pi}{4} + K_1 \sin \frac{\pi}{8}\right)$$

Using the identity $\eta = \cos \varphi$, equation (A3) may be written as a function of η.

The equation is then in the form

$$K(\eta) = \sqrt{1-\eta^2} \sum_{n=0}^{3} a_{2n}\, \eta^{2n} \qquad (A4)$$

where in terms of the coefficients K_n

$$a_0 = K_4$$

$$a_2 = -10\ (K_4 - 1.26\ 173\ K_3 + 0.28284\ K_2 - 0.08966\ K_1)$$

$$a_4 = 24\ (K_4 - 1.66736\ K_3 + 0.94281\ K_2 - 0.32984\ K_1)$$

$$a_6 = -16\ (K_4 - 1.84776\ K_3 + 1.41422\ K_2 - 0.76536\ K_1)$$

---

[1] Where the loading coefficients, K_4, K_3, K_2, and K_1 are at the span stations $\eta = 0$, 0.3827, 0.7071, and 0.9239, respectively.

By a method similar to that employed in reference 2, equation (A2) may be reduced to

$$K(\varphi) = \frac{-\sin 8\varphi}{8 \cos \varphi} K_4 - \frac{0.23097 \cos \varphi \sin 8\varphi}{0.14644 - \cos^2 \varphi} K_3$$

$$+ \frac{0.17678 \cos \varphi \sin 8\varphi}{0.5000 - \cos^2 \varphi} K_2 - \frac{0.09567 \cos \varphi \sin 8\varphi}{0.85355 - \cos^2 \varphi} K_1 \qquad (A5)$$

The series (A3) was originally obtained by Trefftz and was used in this form by Mutterperl. (See reference 1.) Prandtl and Betz originally gave the loading series in the form of equation (A4), which is the type of series used by Falkner. (See reference 1.)

Equation (A5) has been derived and is presented herein to provide a simple means for obtaining loading coefficients at spanwise stations other than the four covered by the Weissinger method. Values of loading coefficient are obtained directly by the Weissinger method for the spanwise stations $\eta = 0$, 0.3827, 0.7071, and 0.9239. Through use of the following procedure, which is based on equation (A5), values of loading coefficient can also be obtained for the spanwise stations $\eta = 0.1951$, 0.5555, and 0.8314.

Equation (A5) can be written for specific values of φ as

$$K_k = \sum_{n=1}^{4} a_{nk} K_n \qquad (A6)$$

where k represents odd number integers giving span stations between those given by n $\left(\text{since } \eta_n = \cos \frac{n\pi}{8} \text{ and } n_k = \cos \frac{k\pi}{16}\right)$ and K_k is the value of the loading coefficient at the span station k. The values of the coefficients a_{nk} are given by

$$a_{1k} = \frac{-0.09567 \cos \frac{k\pi}{16} \sin \frac{k\pi}{2}}{0.85355 - \cos^2 \frac{k\pi}{16}}$$

$$a_{2k} = \frac{0.17678 \cos \frac{k\pi}{16} \sin \frac{k\pi}{2}}{0.500 - \cos^2 \frac{k\pi}{16}}$$

$$a_{3k} = \frac{-0.23097 \cos \frac{k\pi}{16} \sin \frac{k\pi}{2}}{0.14644 - \cos^2 \frac{k\pi}{16}}$$

$$a_{4k} = \frac{- \sin \frac{k\pi}{2}}{8 \cos \frac{k\pi}{16}}$$

Since these coefficients are a function only of the integers n and k they may be tabulated as follows and used for any plan form:

a_{nk}			
η	0.8314	0.5555	0.1951
n \ k	3	5	7
1	.4898	-.0976	.0229
2	.7684	.5135	-.0747
3	-.3524	.7900	.4159
4	.1503	-.2250	.6407

Although it is possible to evaluate a_{nk} and hence K_k for $k = 1$, the terms for $k = 1$ have been omitted since in practice a value of K at this point ($\eta = 0.9808$) is of little use in fairing a loading curve.

Thus to find the loading coefficient for an intermediate point η_k, it is necessary to (1) substitute into equation (A6) the appropriate values of a_{nk} from the foregoing table, and the values of K_n obtained from the Weissinger method and (2) evaluate the summation.

REFERENCES

1. Van Dorn, Nicholas H., and DeYoung, John: A Comparison of Three Theoretical Methods of Calculating Span Load Distribution on Swept Wings. NACA RRM No. A7C31, 1947.

2. Multhopp, H.: Die Berechnung der Augtriebsverteilung von Tragflügeln. Luftf.-Forschg., Bd. 15 (1938).

3. Swanson, Robert S., and Priddy, E. LaVerne: Lifting-Surface-Theory Values of the Damping in Roll and of the Parameter Used in Estimating Aileron Stick Forces. NACA ARR No. L5F23, 1945.

4. Krienes, Klaus: The Elliptic Wing Based on the Potential Theory. NACA TM No. 971, 1941.

5. Jones, Robert T.: Properties of Low-Aspect-Ratio Pointed Wings at Speeds Below and Above the Speed of Sound. NACA TN No. 1032, 1946.

6. Zimmerman, C.H.: Characteristics of Clark Y Airfoils of Small Aspect Ratios. NACA Rep. No. 431, 1932.

7. Lange und Wacke: Prufbericht über Drei und Sechs-Komponentenmessungen an der Zuskitzungsreibe von Flügeln kleiner Streckung (Teilbericht: Dreieckflügel) UM 1023 (Geheim). Nov. 1943.

8. Shortal, Joseph A., and Maggin, Bernard: Effect of Sweepback and Aspect Ratio on Longitudinal Stability Characteristics of Wings at Low Speeds. NACA TN No. 1093, 1946.

9. Weissinger, J.: The Lift Distribution of Swept-Back Wings NACA TM No. 1120, 1947.

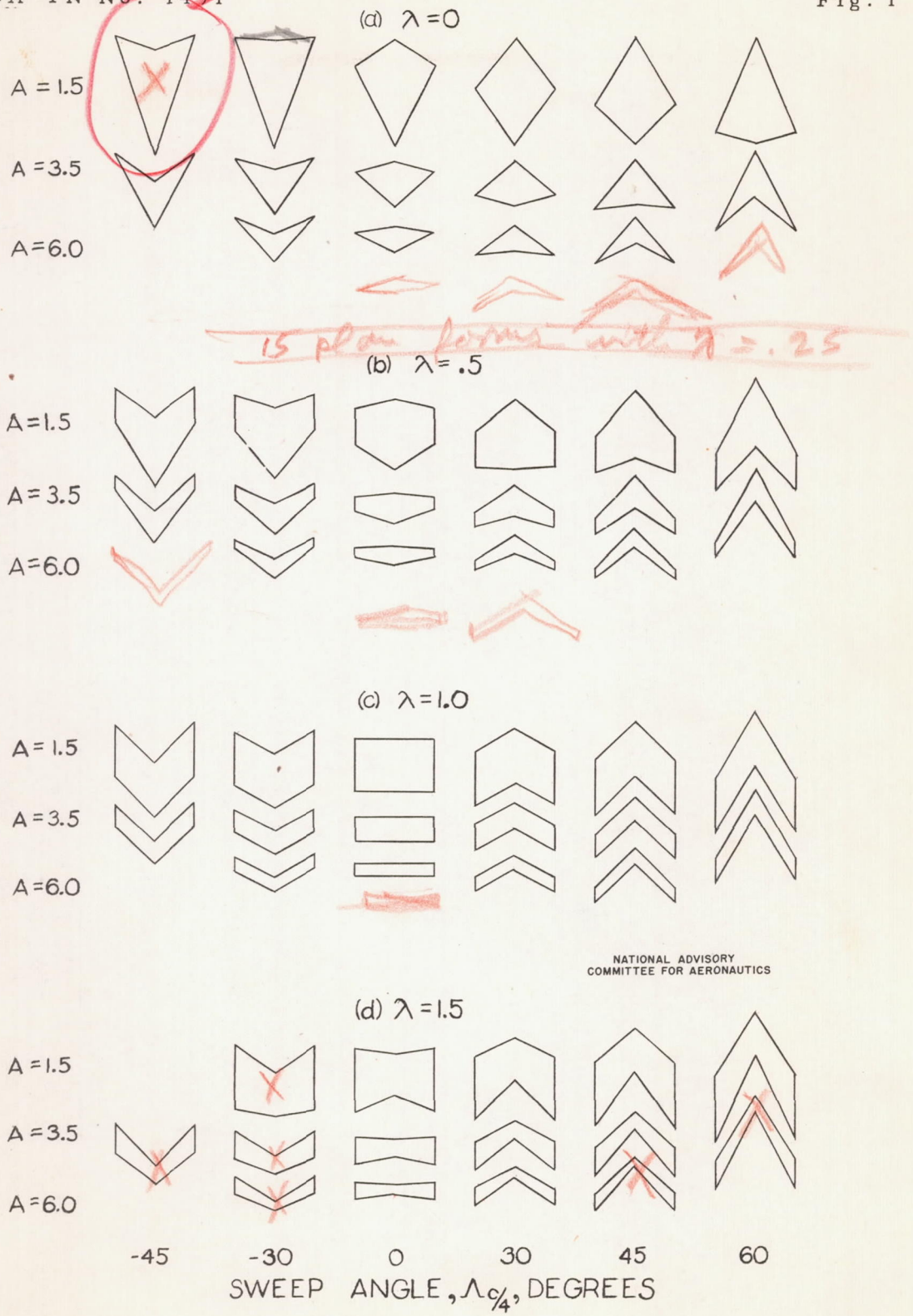

FIGURE 1.- RANGE OF PLAN FORMS INVESTIGATED BY THE WEISSINGER METHOD.

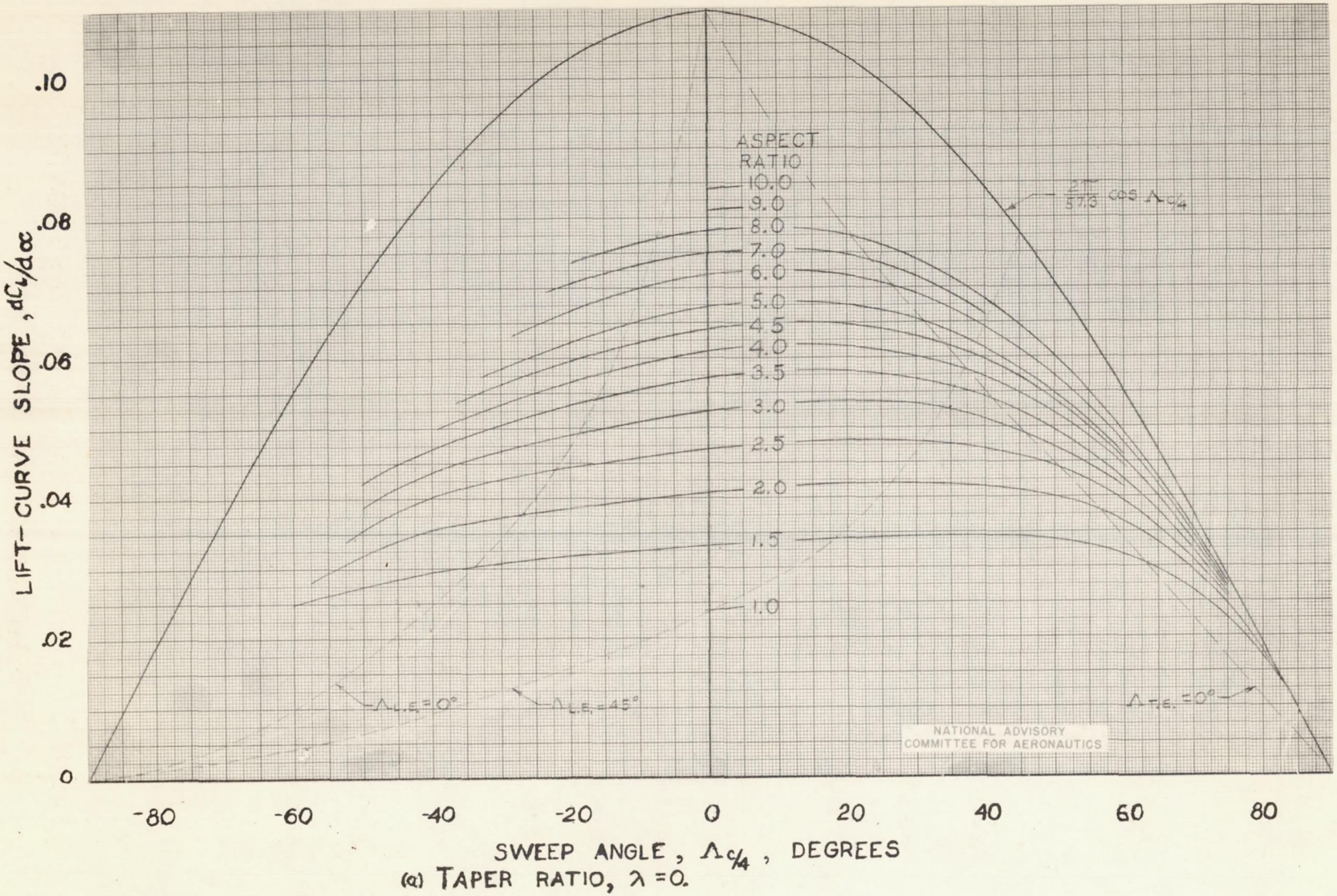

(a) TAPER RATIO, $\lambda = 0$.

FIGURE 2- VARIATION OF LIFT-CURVE SLOPE WITH SWEEP FOR VARIOUS ASPECT RATIOS. AND TAPER RATIOS.

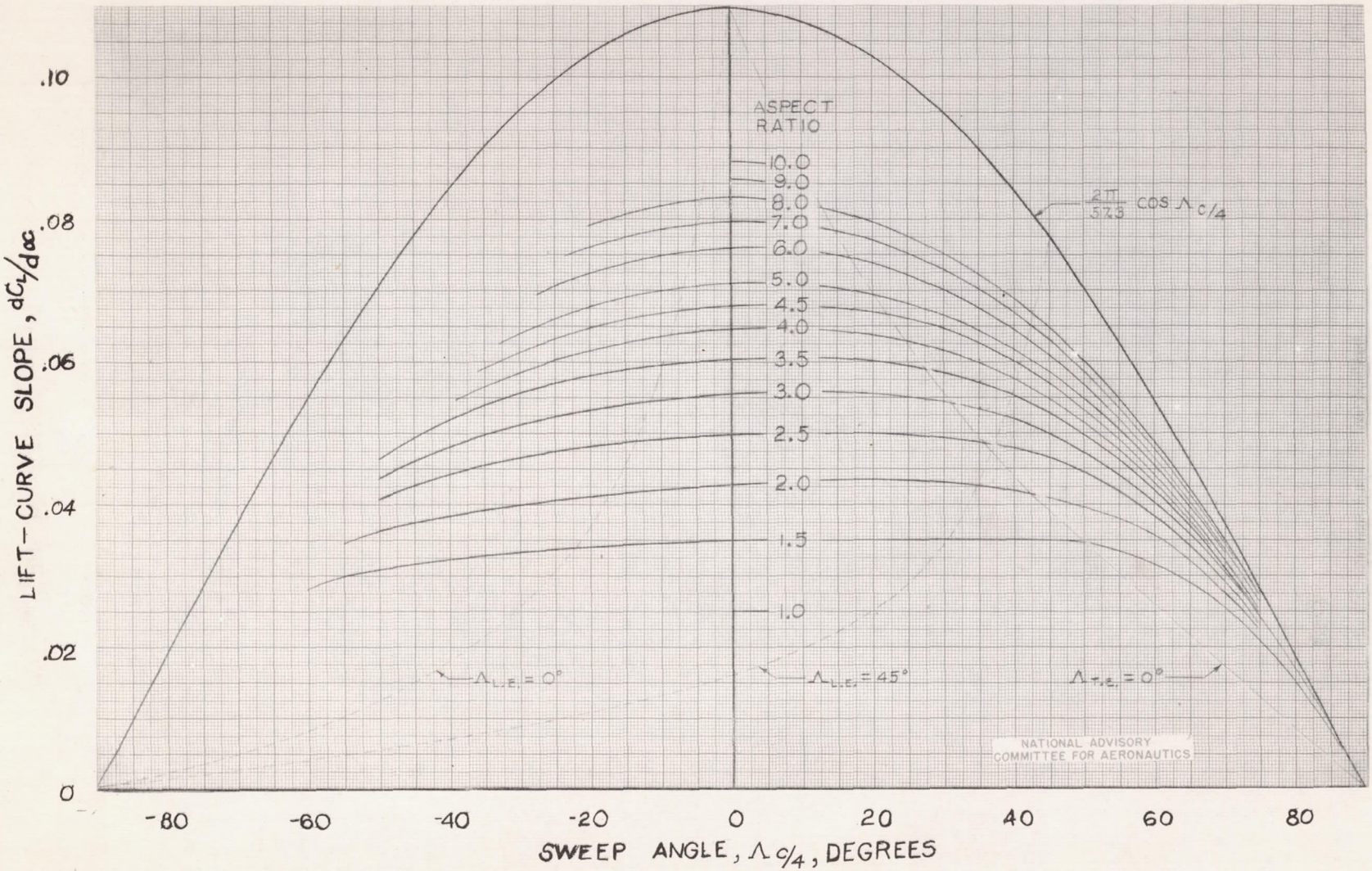

(b) TAPER RATIO, $\lambda = .25$.

FIGURE 2.- CONTINUED.

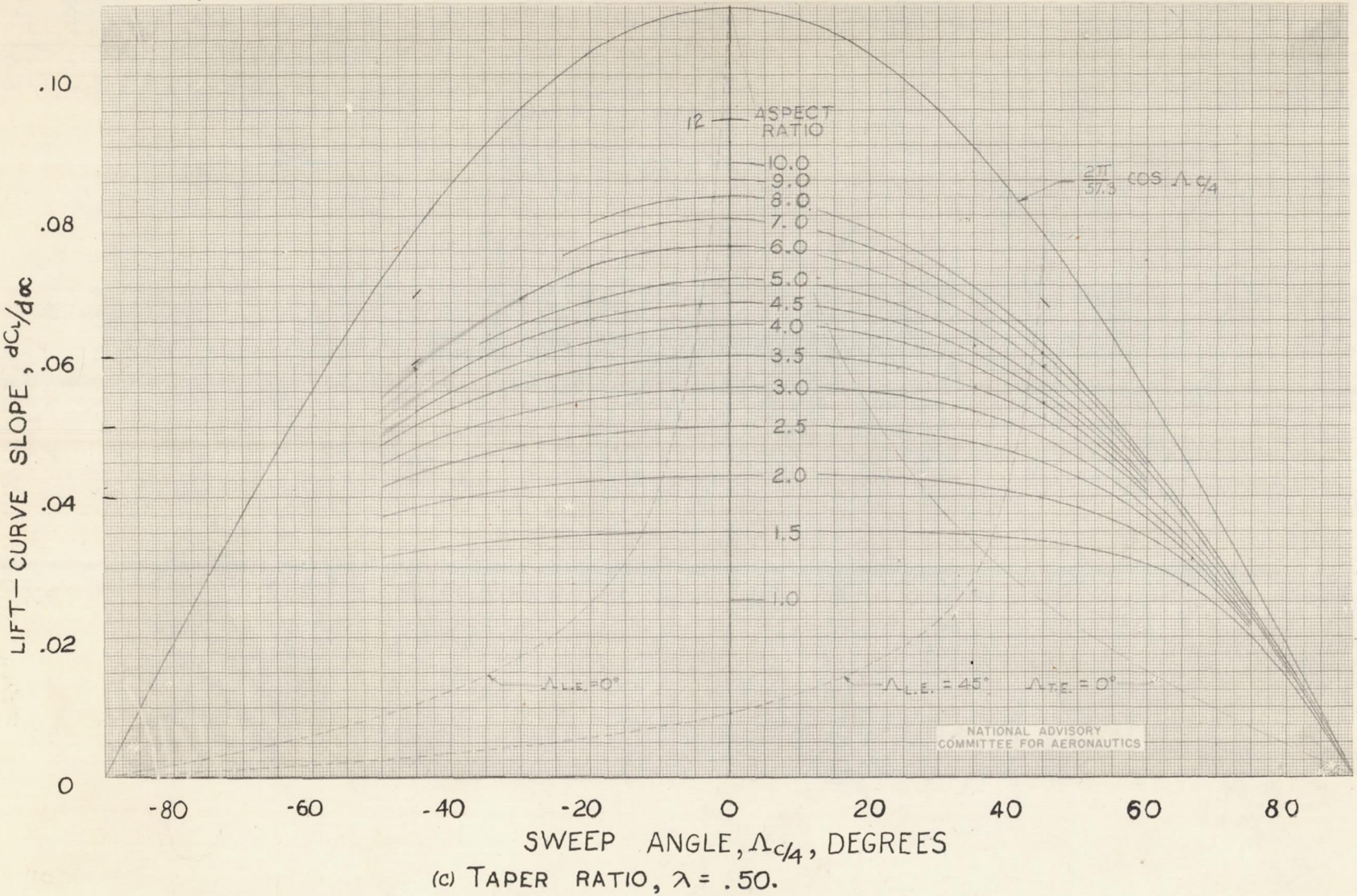

(c) TAPER RATIO, $\lambda = .50$.

FIGURE 2.— CONTINUED.

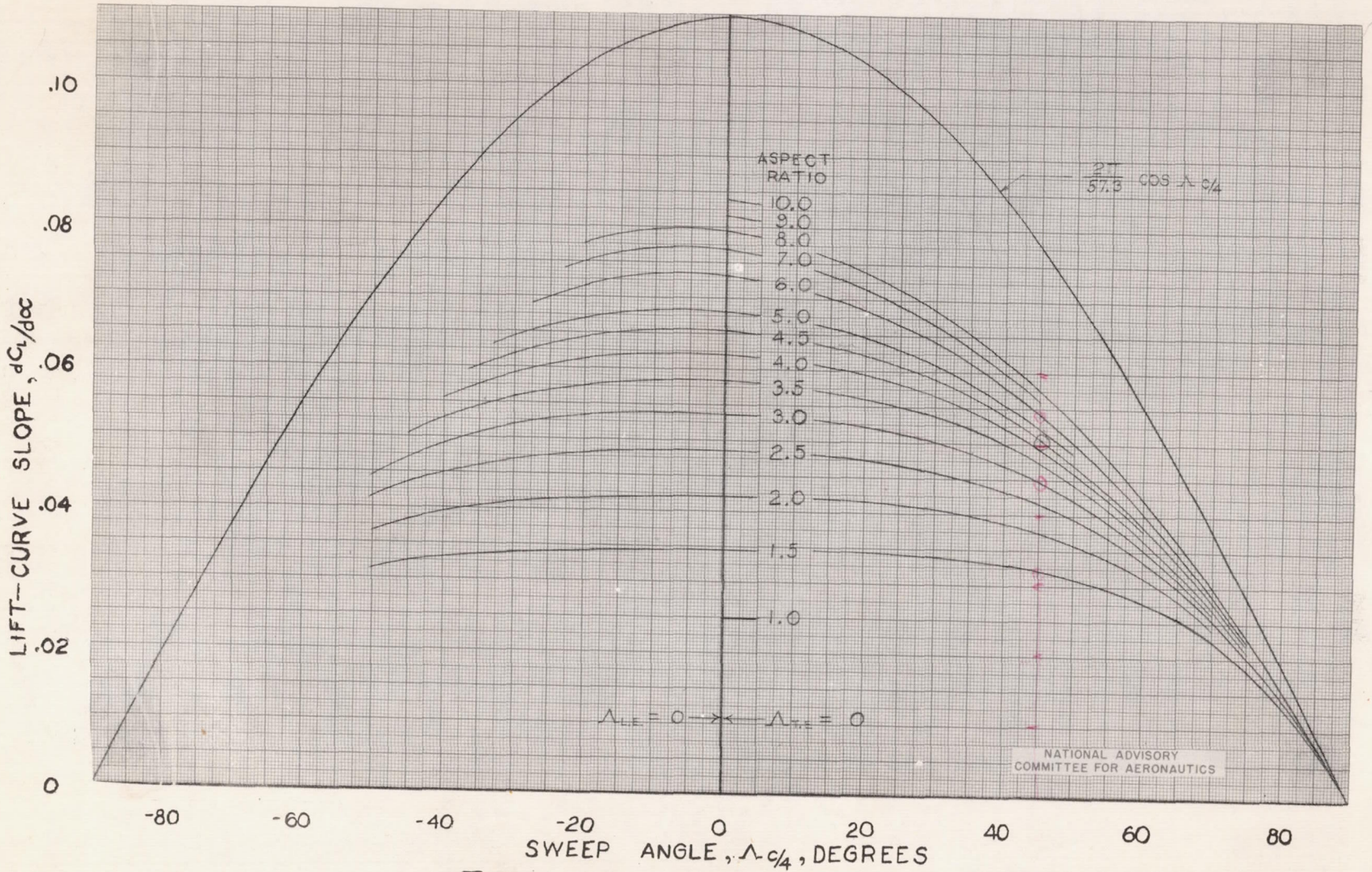

(d) TAPER RATIO, $\lambda = 1.0$.

FIGURE 2- CONTINUED.

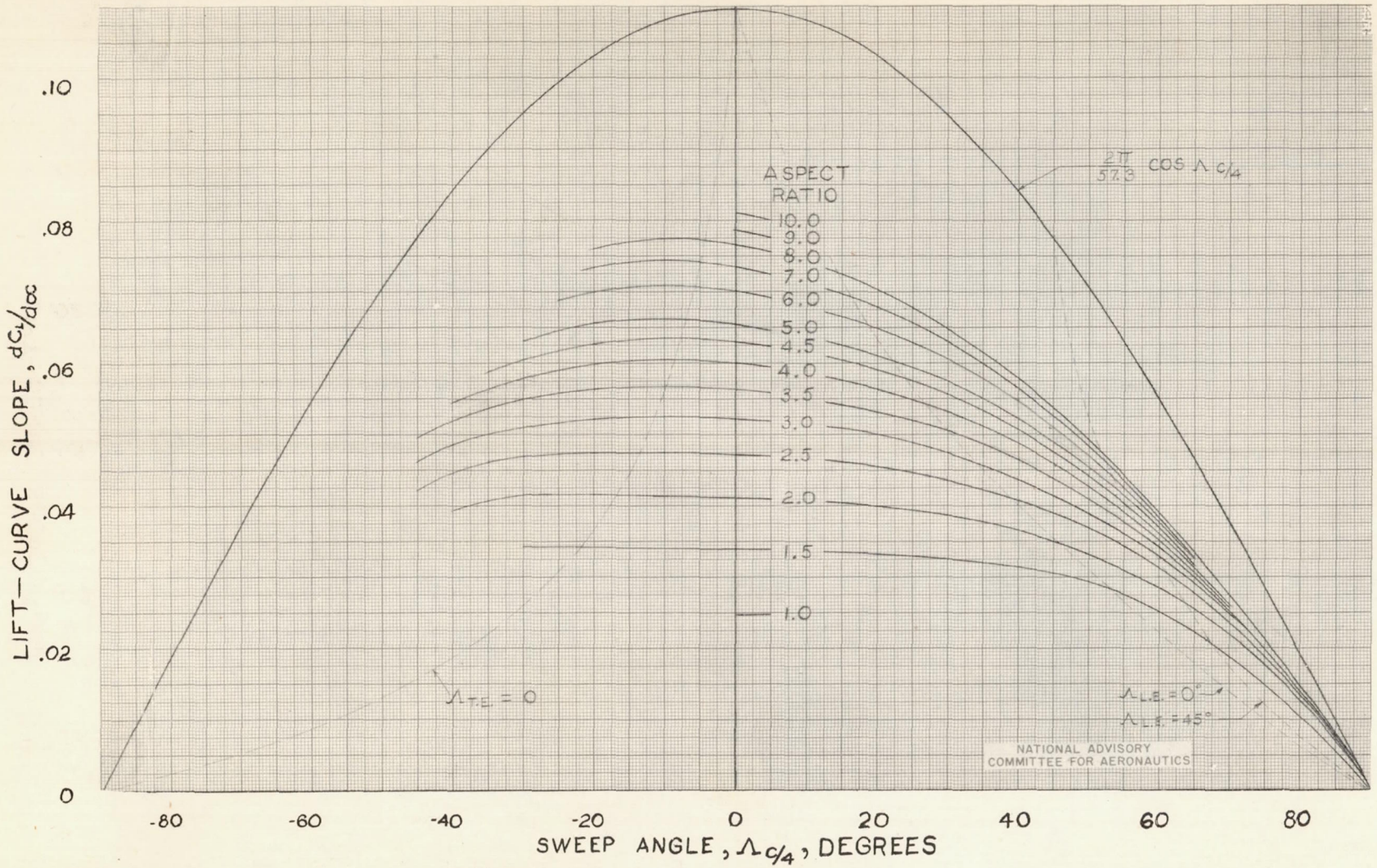

(e) TAPER RATIO, $\lambda = 1.5$.

FIGURE 2.— CONCLUDED.

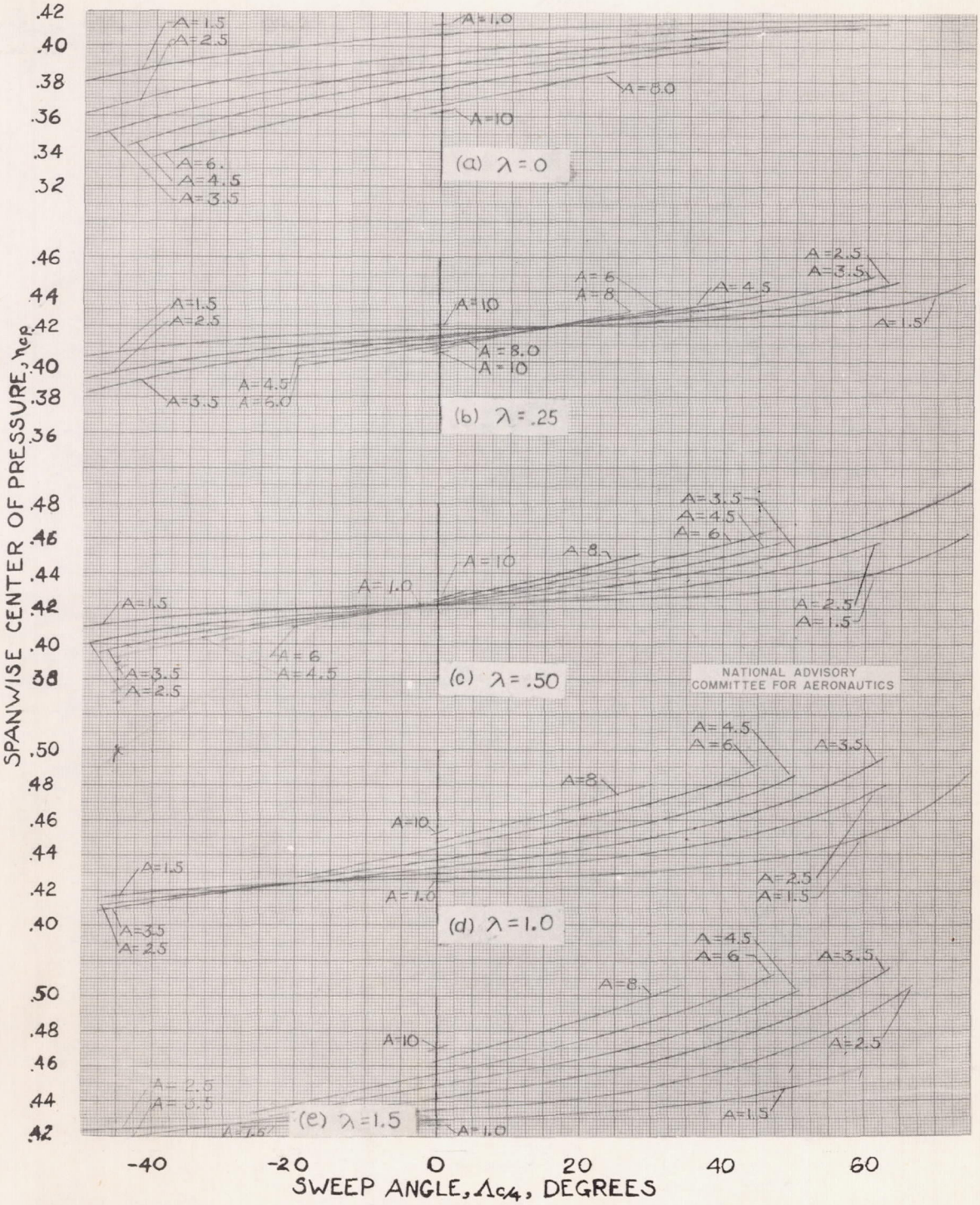

FIGURE 3.- VARIATION OF SPANWISE CENTER OF PRESSURE WITH SWEEP FOR VARIOUS ASPECT RATIOS AND TAPER RATIOS.

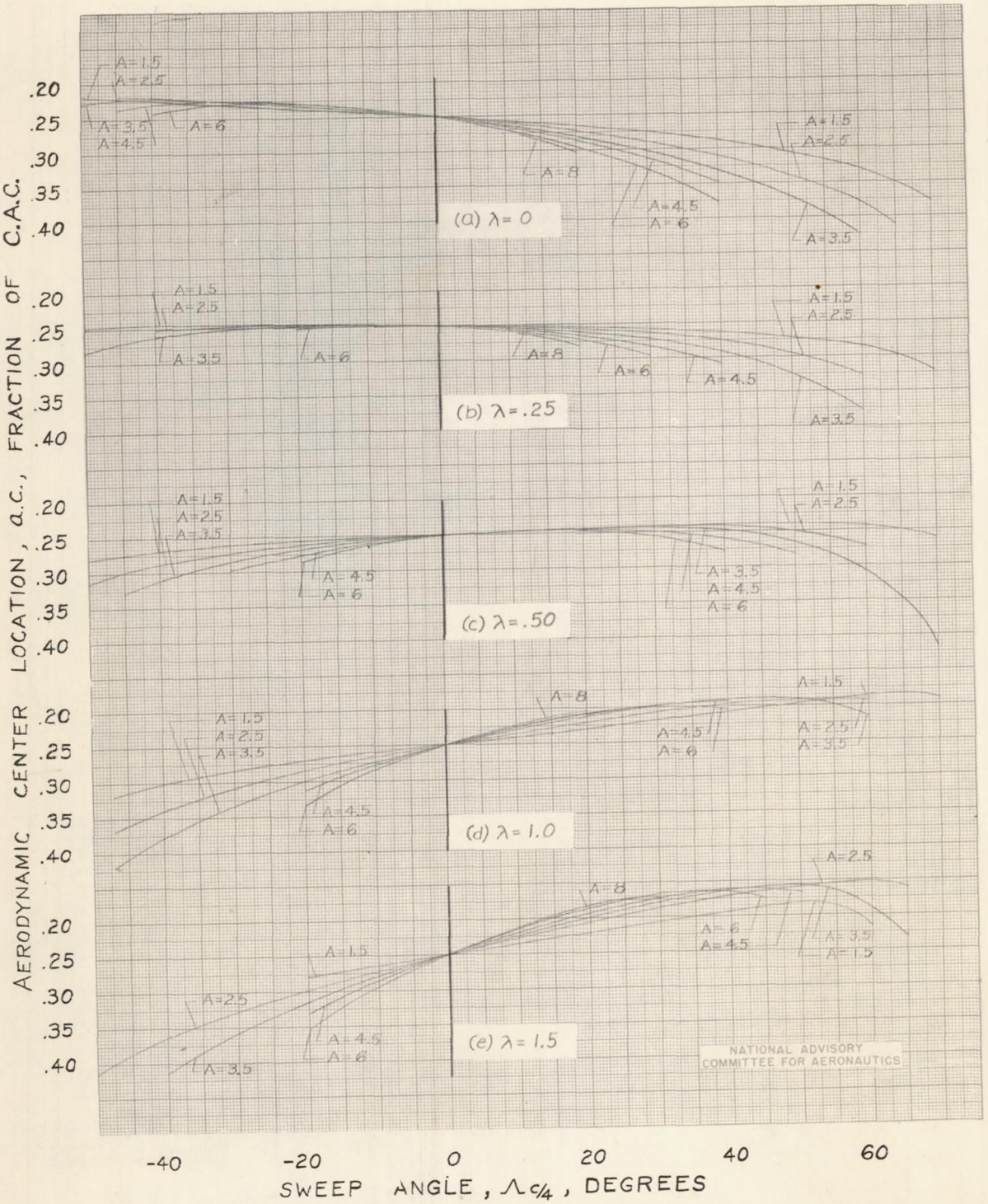

FIGURE 4.- VARIATION OF AERODYNAMIC CENTER LOCATION WITH SWEEP FOR VARIOUS ASPECT RATIOS AND TAPER RATIOS.

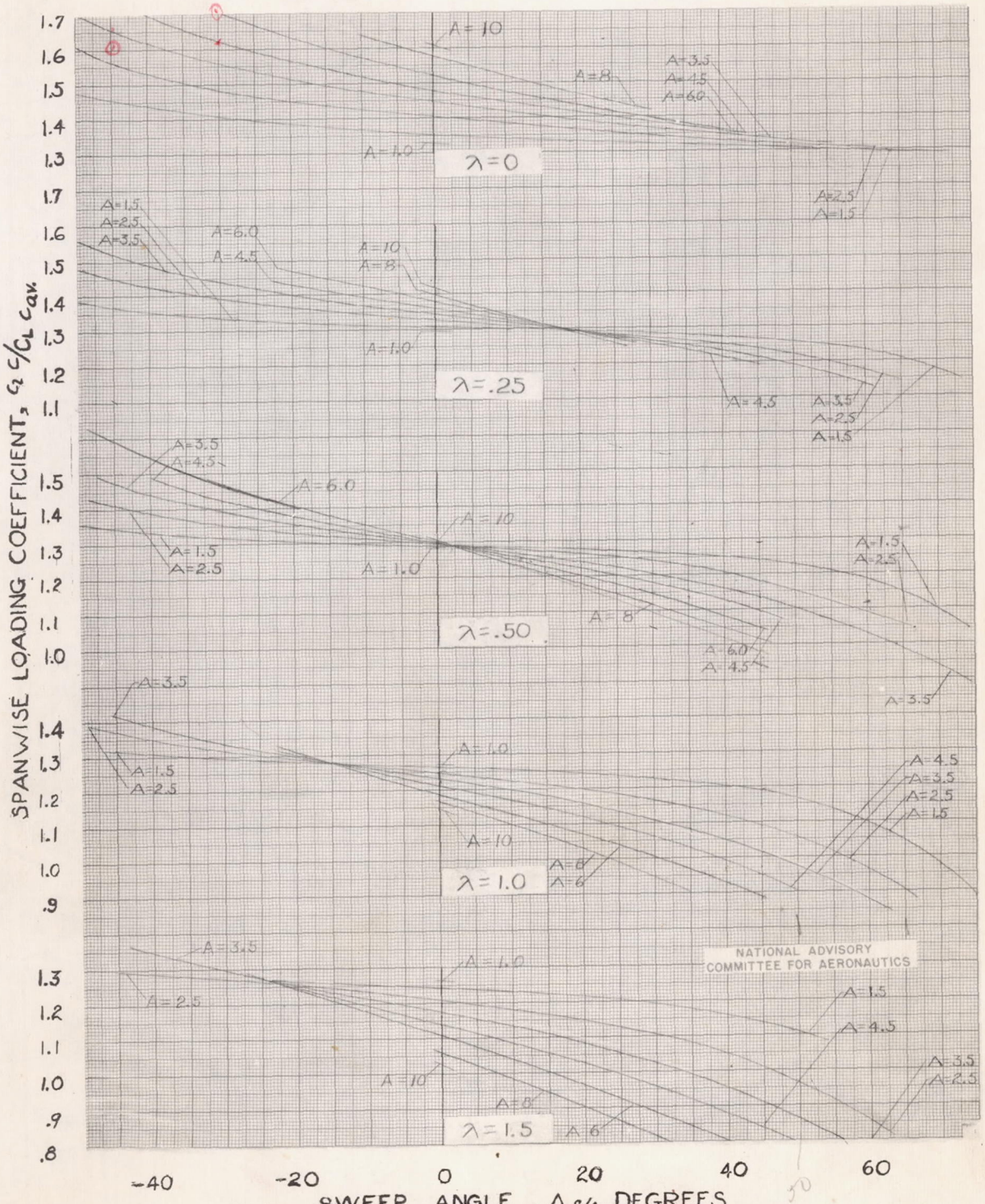

(a) FRACTION OF SEMISPAN, $\eta = 0$

FIGURE 5.- VARIATION OF SPANWISE LOADING COEFFICIENT WITH SWEEP FOR VARIOUS ASPECT RATIOS AND TAPER RATIOS.

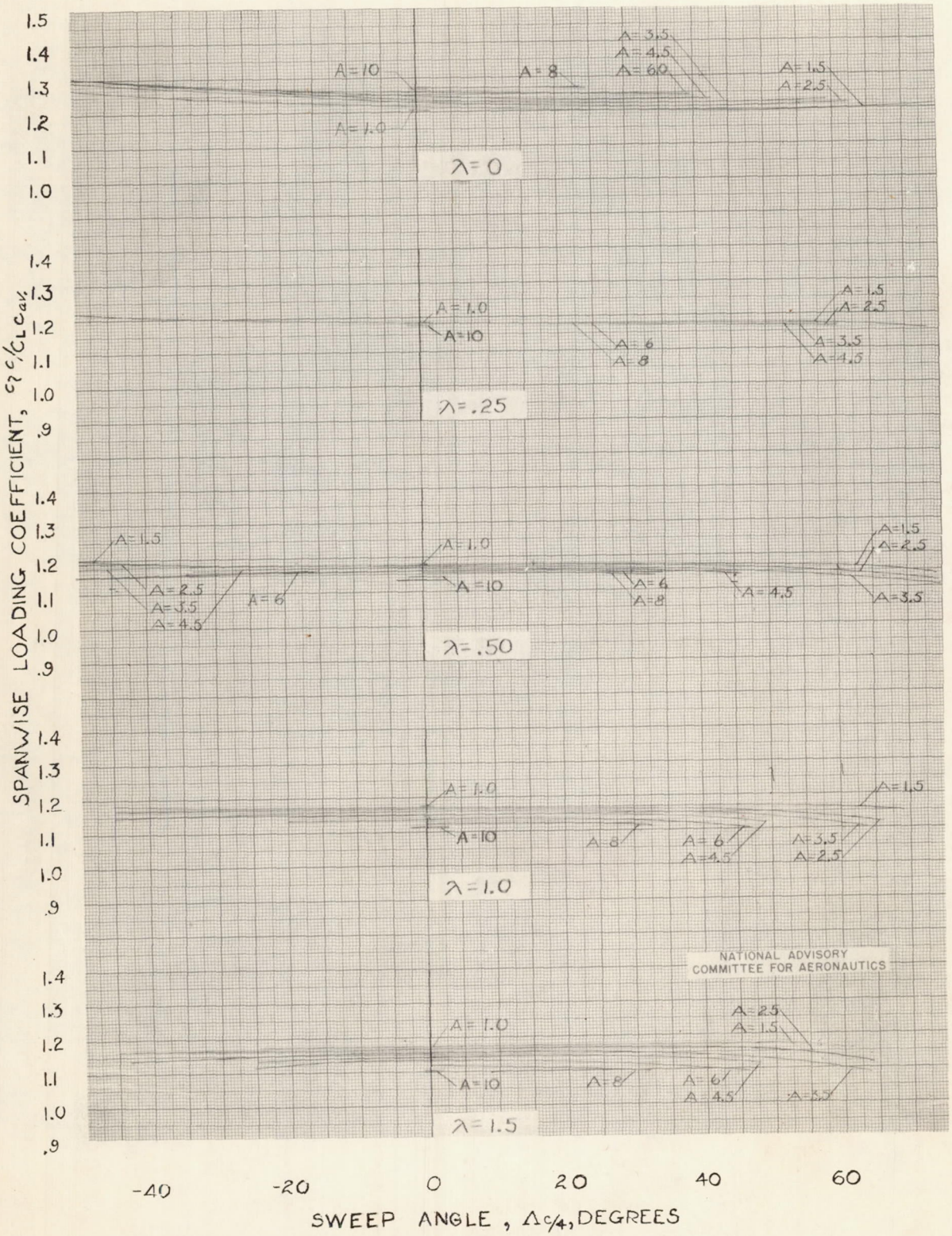

(b) FRACTION OF SEMISPAN, $\eta = .3827$

FIGURE 5.- CONTINUED.

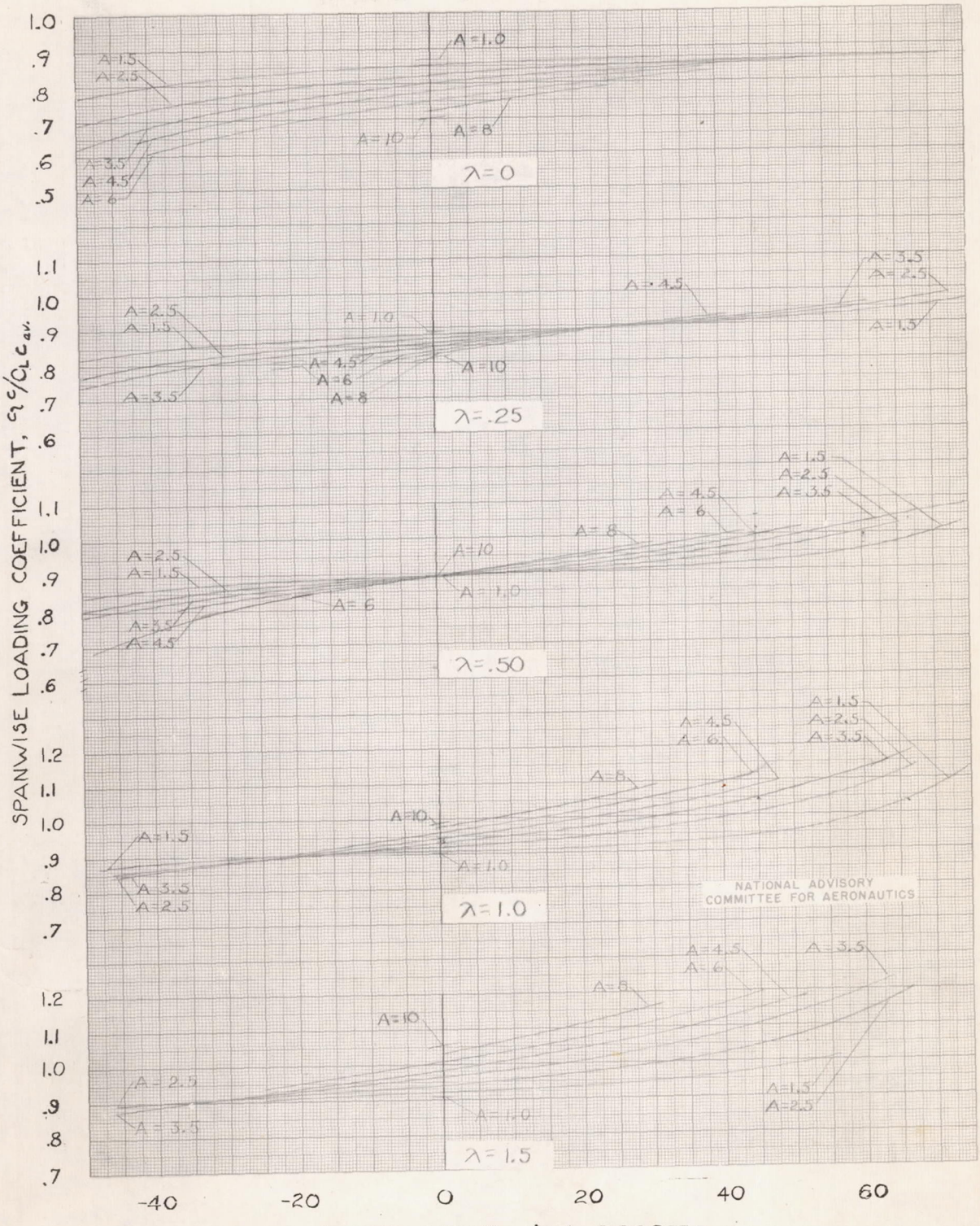

(c) FRACTION OF SEMISPAN, η=.7071.

FIGURE 5.- CONTINUED

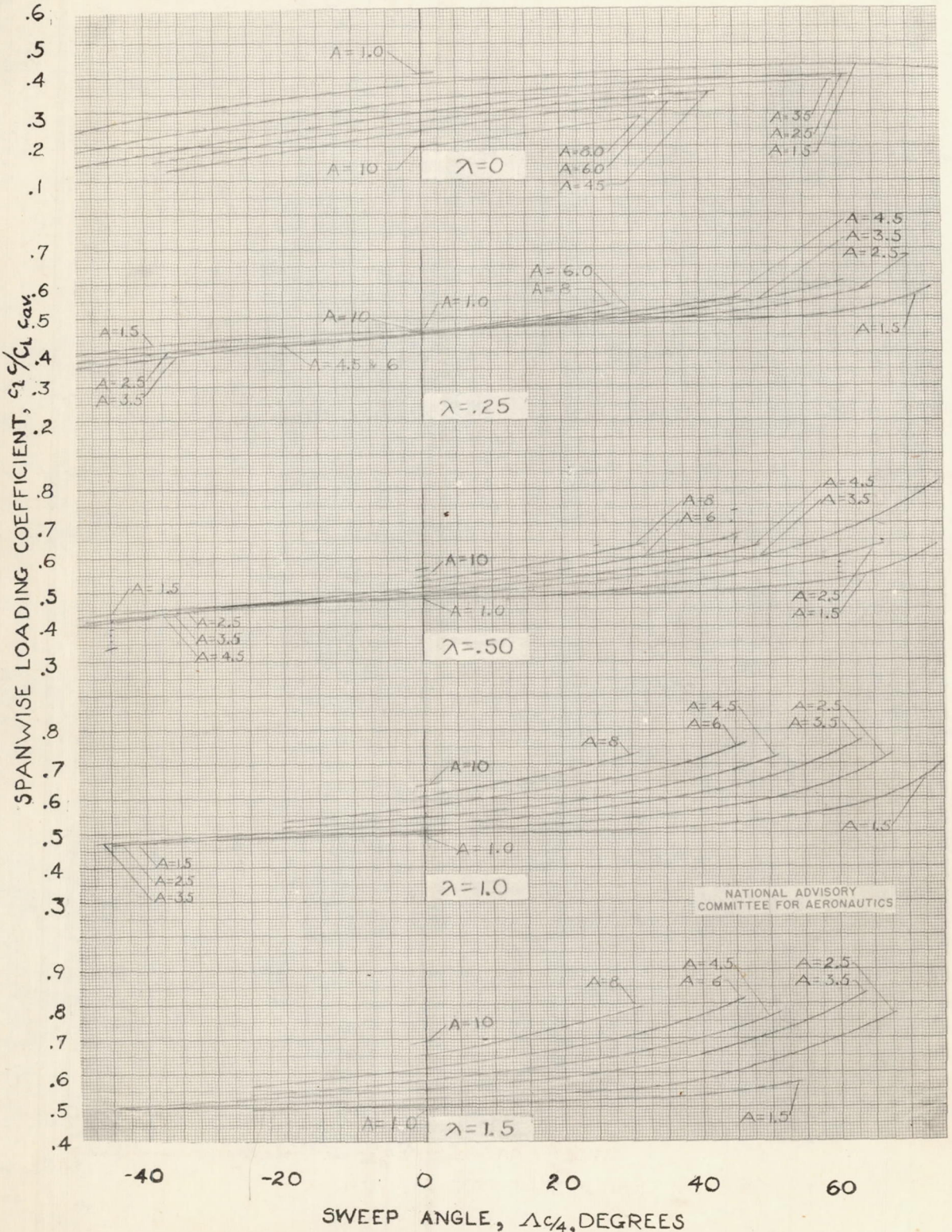

(d) FRACTION OF SEMISPAN, η=.9239.

FIGURE 5.- CONCLUDED.

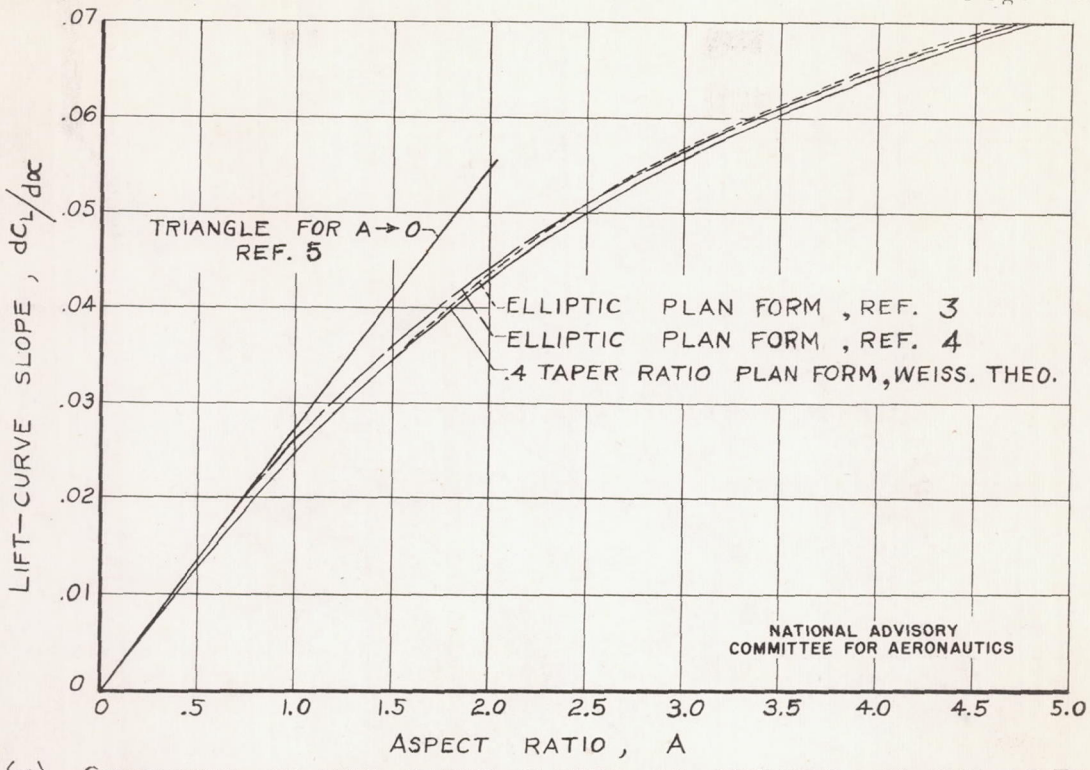

(a) Comparison of lift-curve slopes as obtained by the lifting line method with those obtained by the lifting surface methods of references 4 and 5.

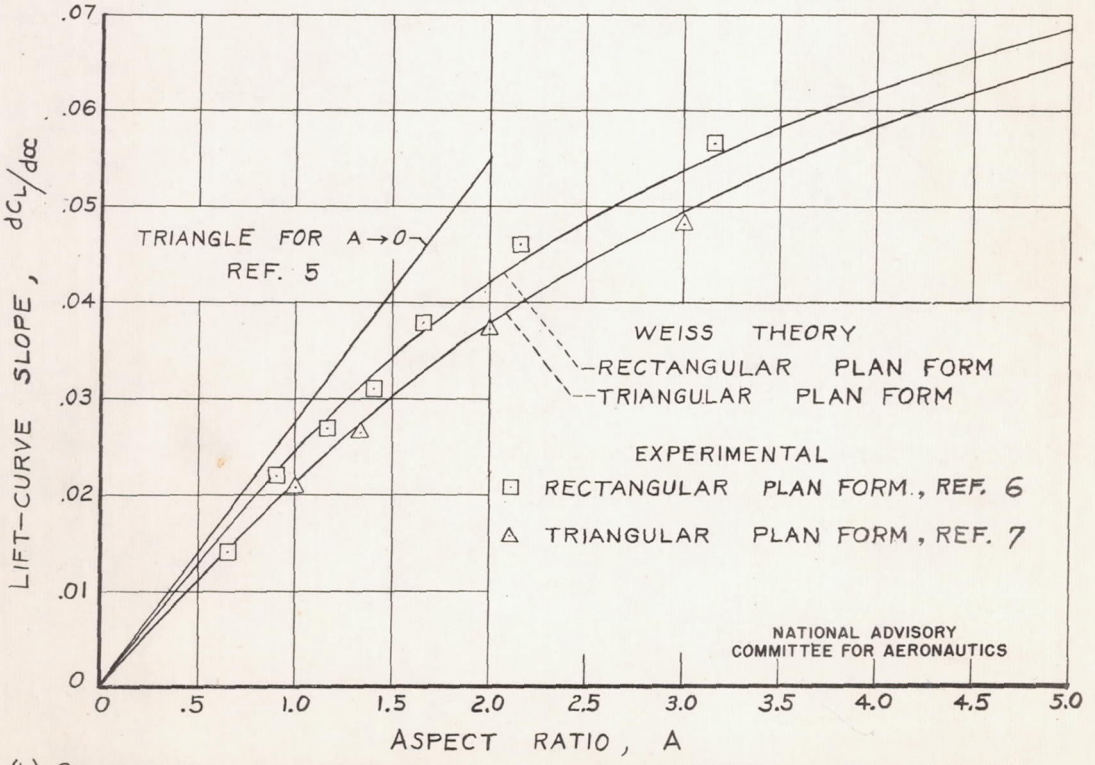

(b) Comparison of theoretical and experimental lift-curve slopes for rectangular and triangular wings.

Figure 6.- Evaluation of Weissinger method for estimating lift-curve slope.

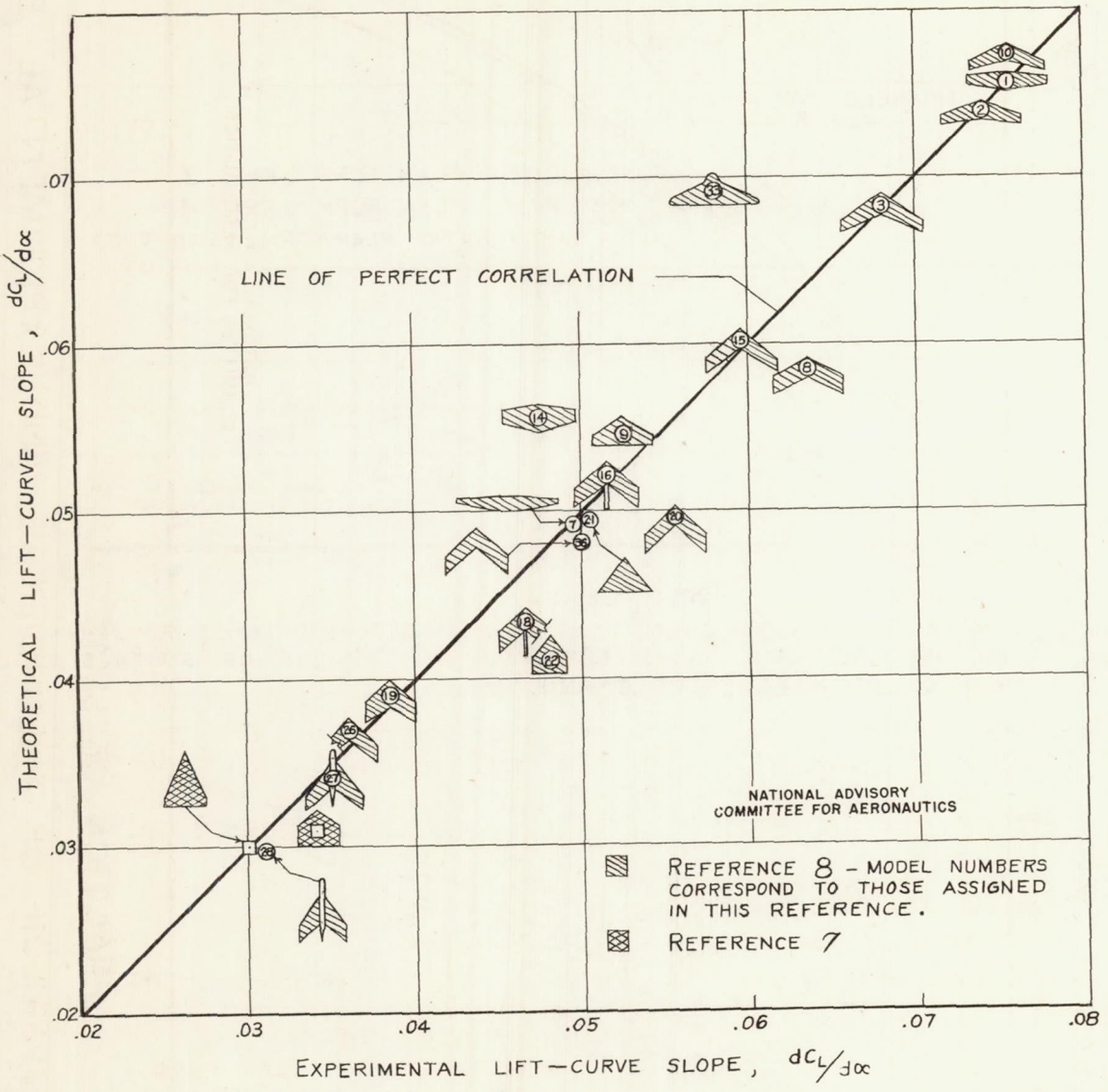

(c) CORRELATION OF THEORETICAL AND EXPERIMENTAL LIFT-CURVE SLOPES FOR VARIOUS PLANFORMS.

FIGURE 6.- CONCLUDED.

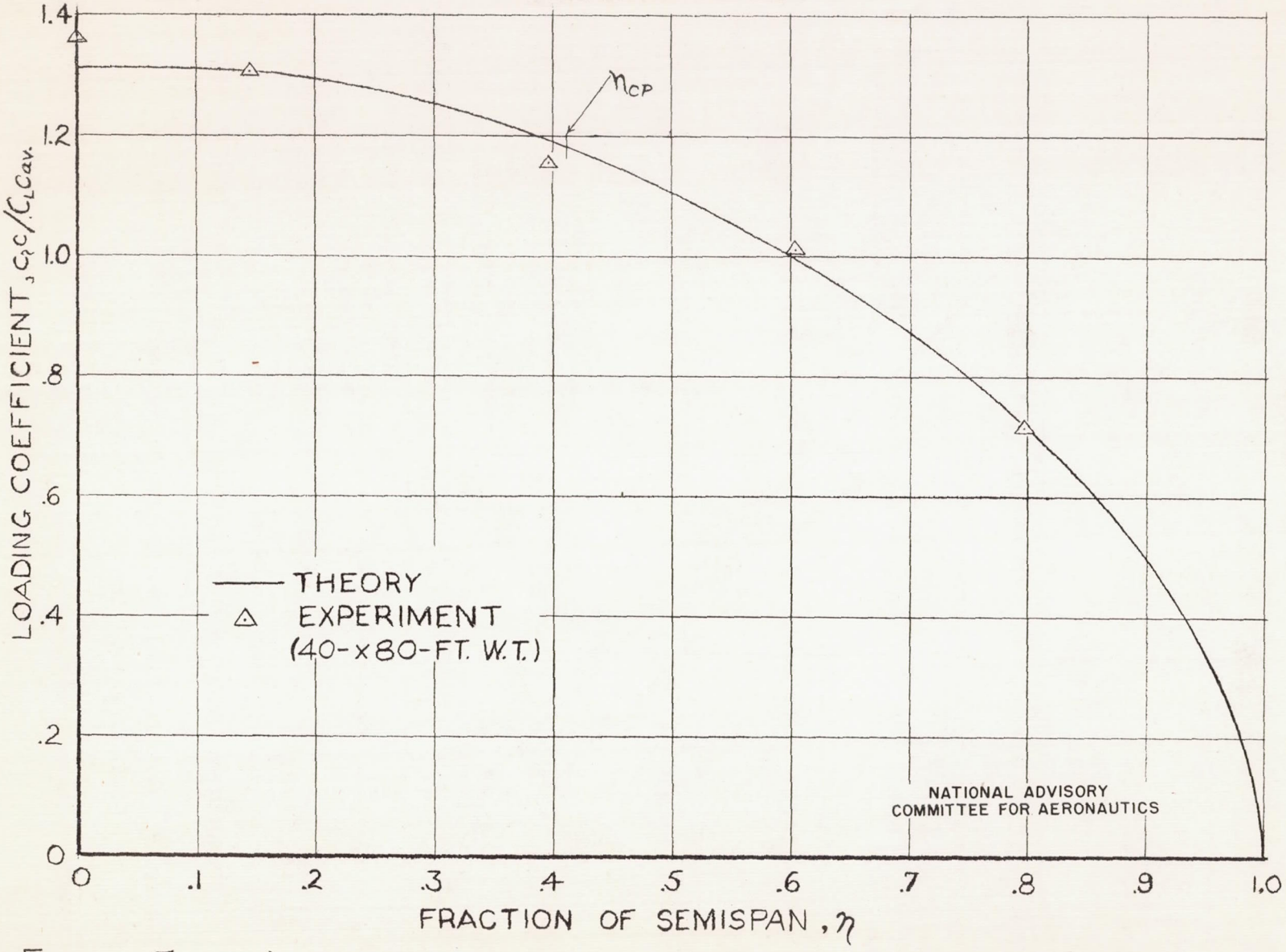

FIGURE 7.- A COMPARISON OF THEORETICAL AND EXPERIMENTAL SPAN LOADING OF A TRIANGULAR WING OF ASPECT RATIO 2.0.

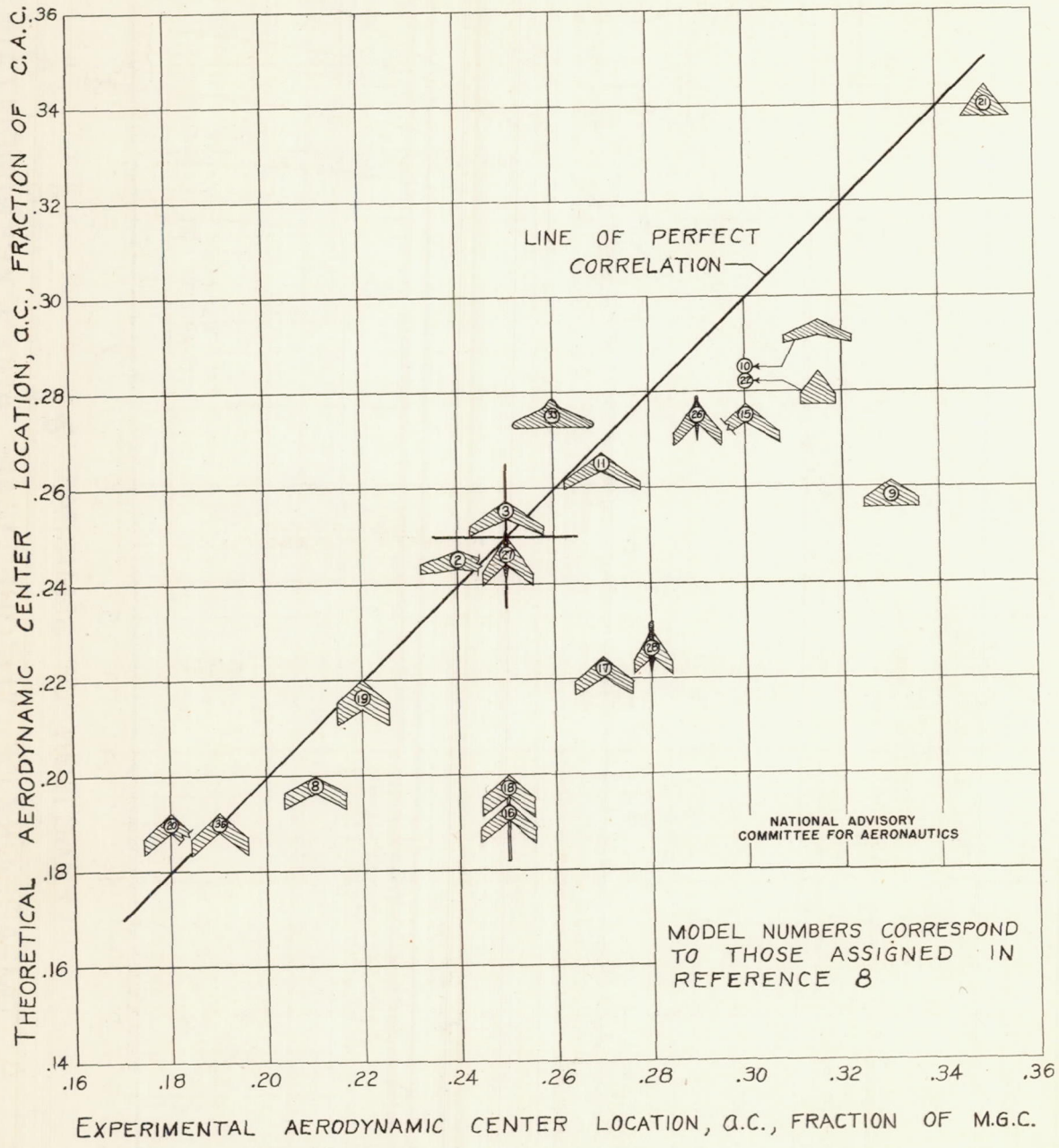

FIGURE 8.- CORRELATION OF THEORETICAL AND EXPERIMENTAL AERODYNAMIC CENTER LOCATIONS

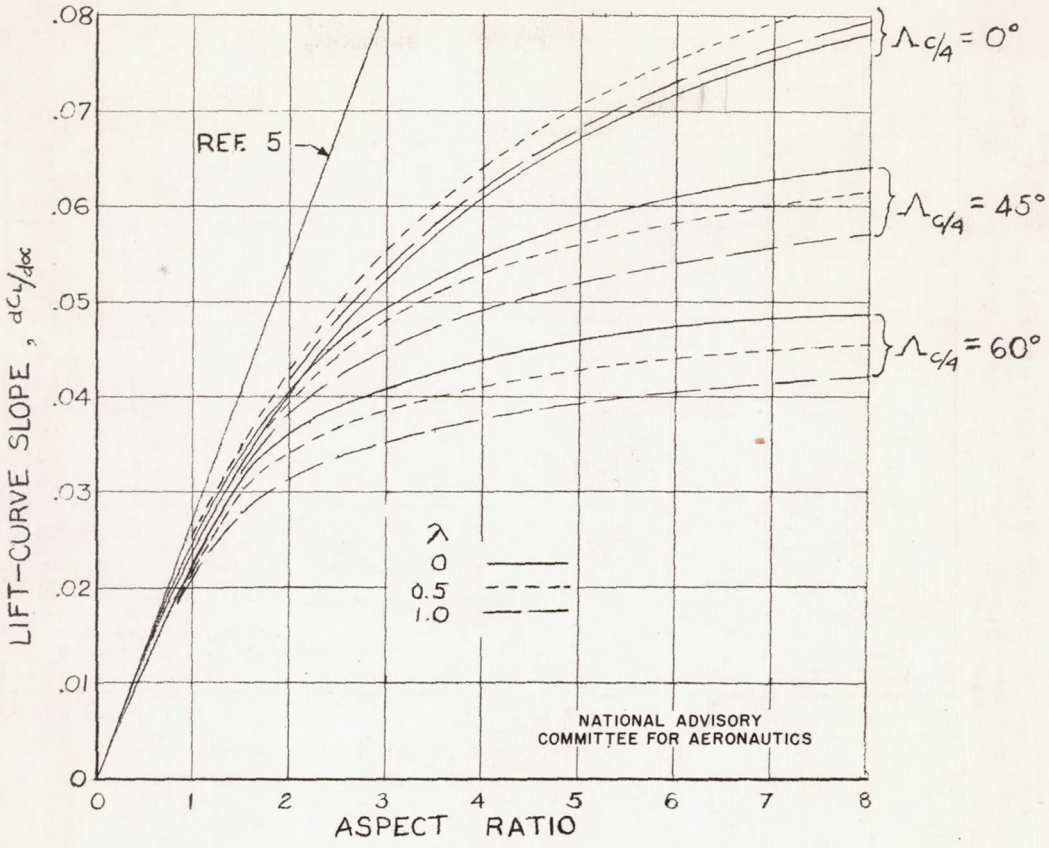

(a). VARIATION OF LIFT-CURVE SLOPE WITH ASPECT RATIO.

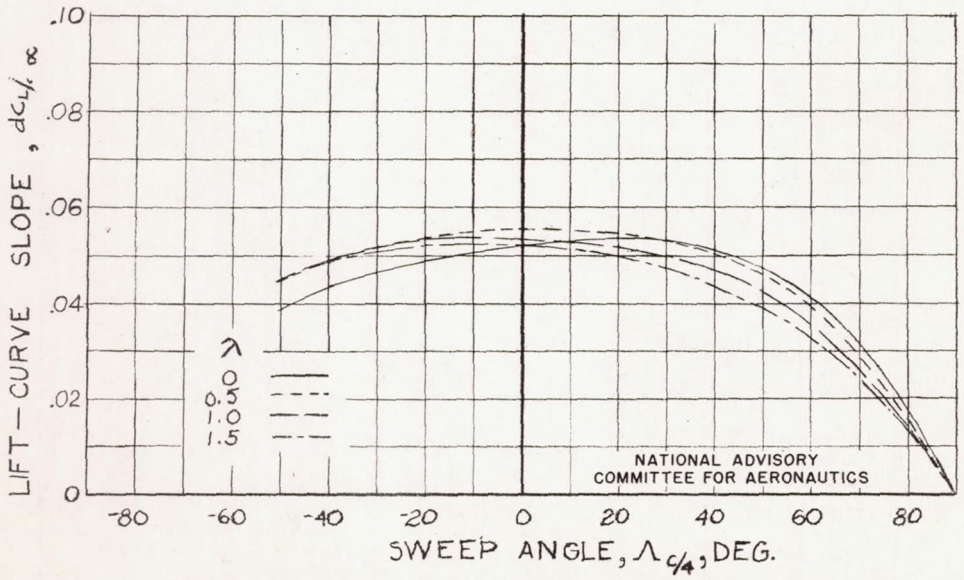

(b) VARIATION OF LIFT-CURVE SLOPE WITH SWEEP ANGLE FOR ASPECT RATIO = 3.0.

FIGURE 9.— EXAMPLES OF THE EFFECT OF WING PLANFORM ON LIFT-CURVE SLOPE.

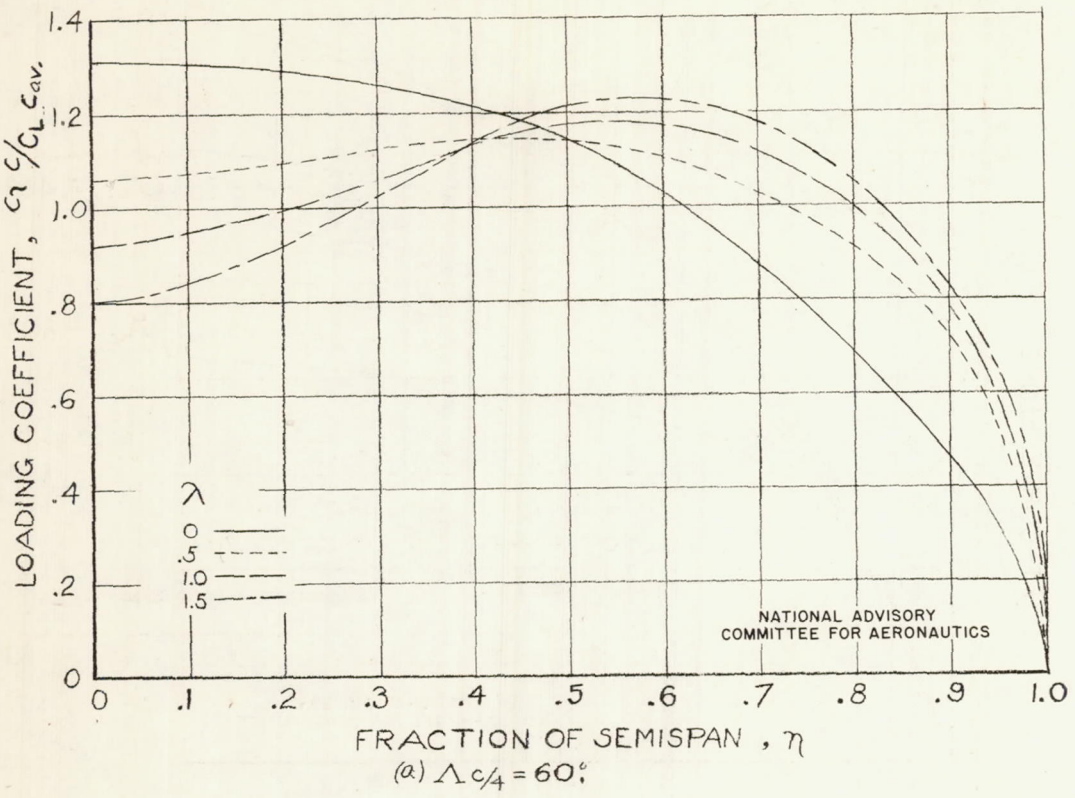

(a) $\Lambda_{c/4} = 60°$

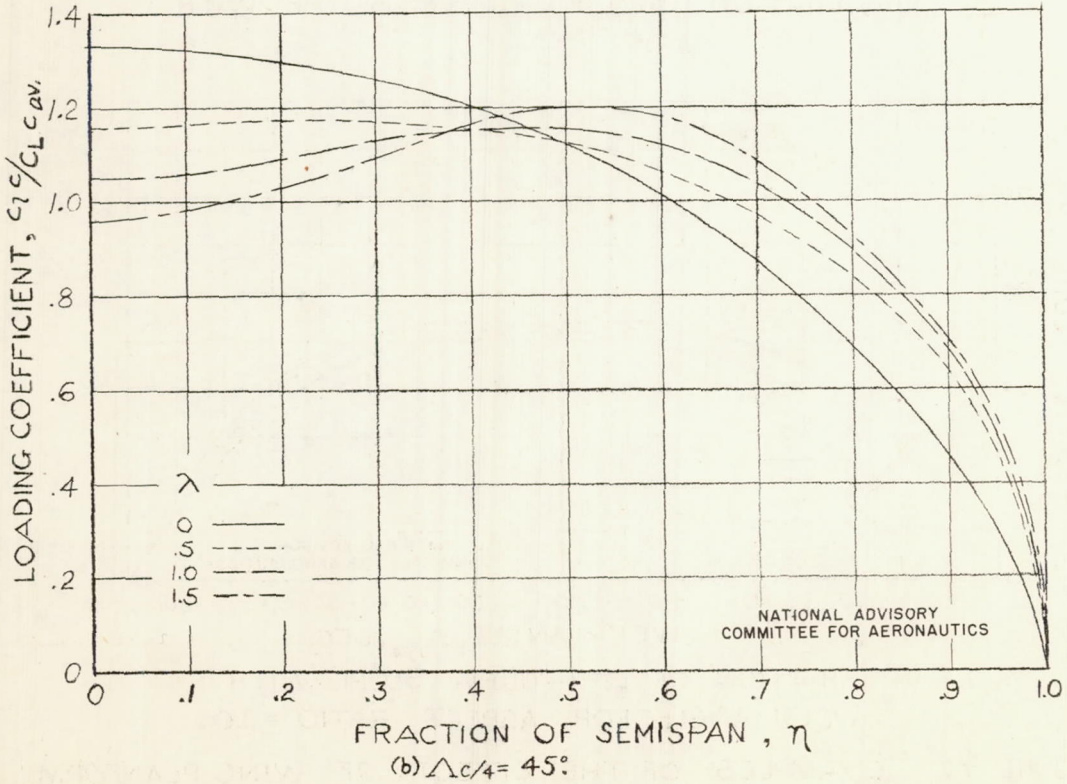

(b) $\Lambda_{c/4} = 45°$

FIGURE 10.- EXAMPLES OF THE EFFECTS OF WING PLANFORM ON THE SPAN LOADING OF A WING OF ASPECT RATIO 3.0.

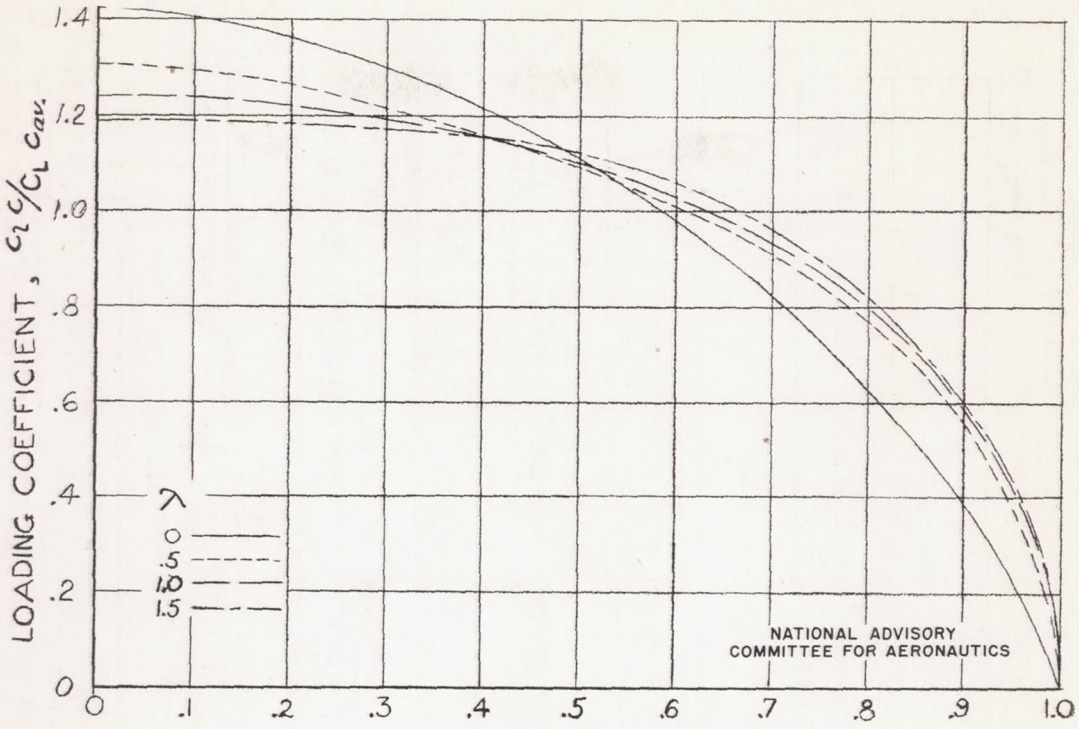

(c) $\Lambda_{c/4}=0°$.

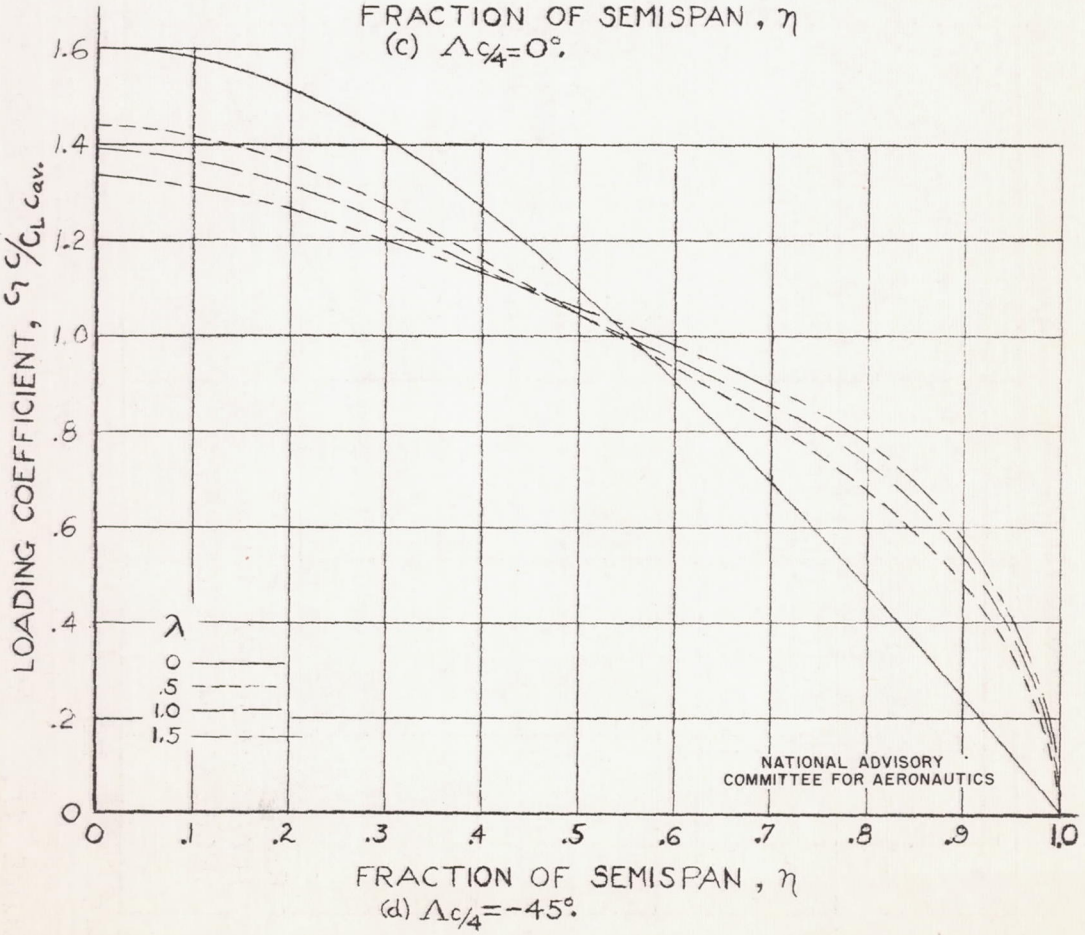

(d) $\Lambda_{c/4}=-45°$.

FIGURE 10.— CONCLUDED.

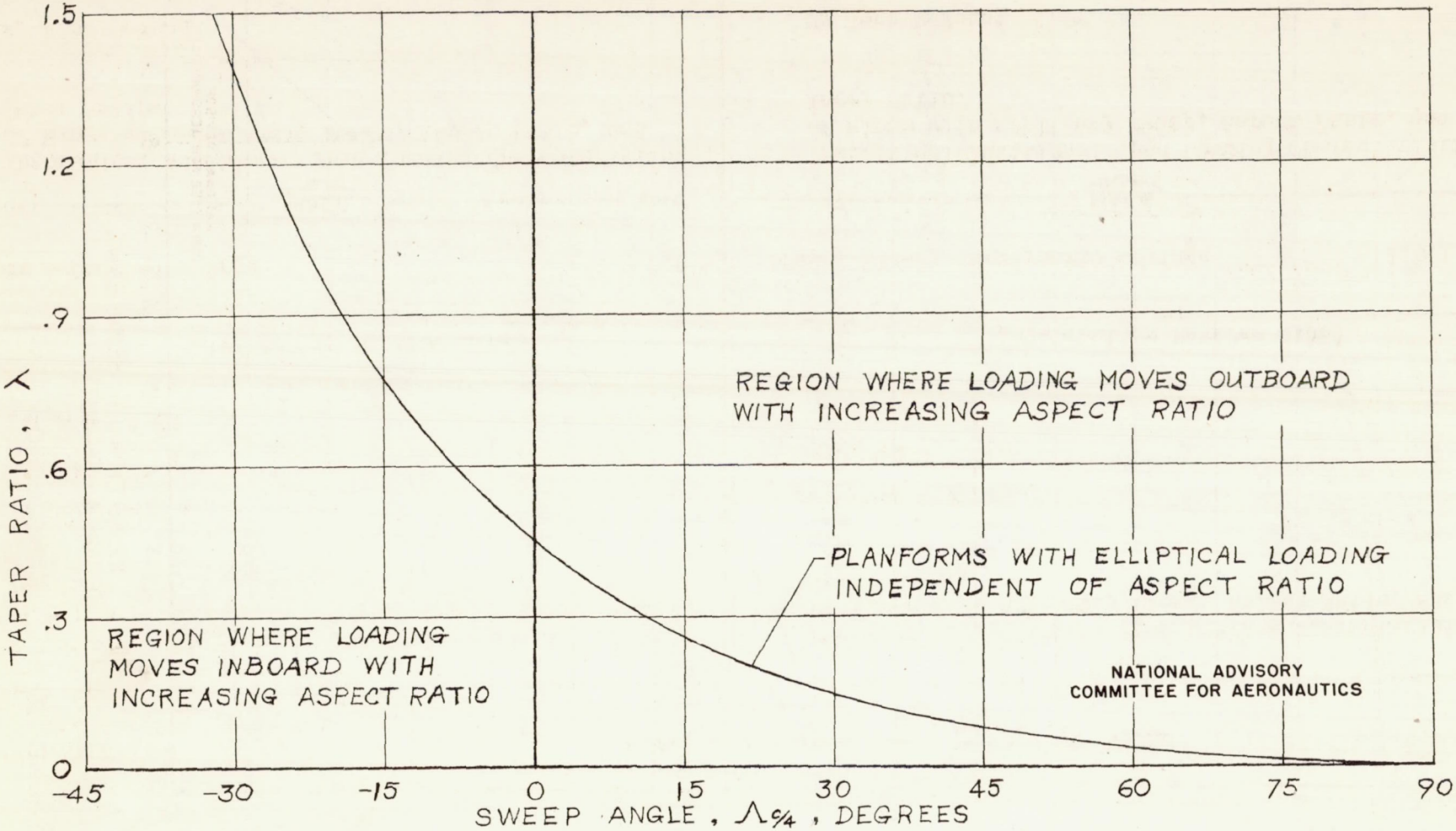

FIGURE 11.— RELATION OF TAPER RATIO AND SWEEP ANGLE REQUIRED FOR ELLIPTICAL LOADING